

SUPPLEMENT TO

LC GC[®]

north america
solutions for separation scientists

Volume 38 Number s6 June 2020
www.chromatographyonline.com



RECENT DEVELOPMENTS IN LC COLUMN TECHNOLOGY

**What does it take to solve
one of the biggest challenges
in chromatography?**



PREMIER

**Be one of the first to see
what PREMIER can do for you.**

waters.com/PREMIER

Waters

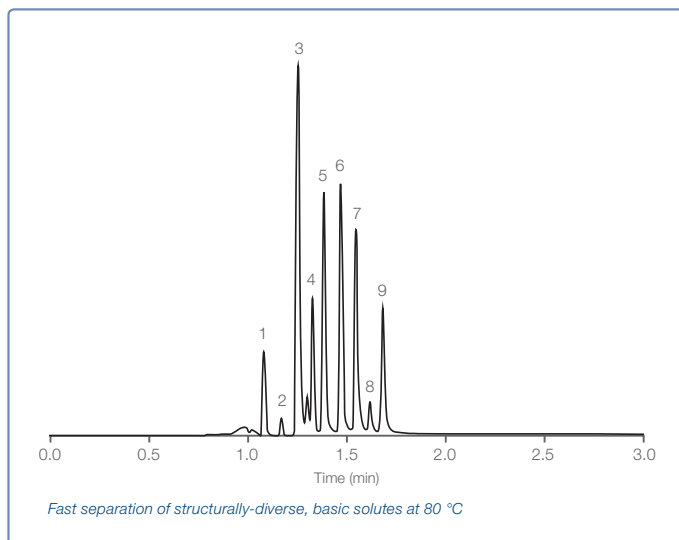
THE SCIENCE OF WHAT'S POSSIBLE.™

High pH and Elevated Temperatures For Fast Separation of Strongly Basic Drug Compounds

Two important but frequently underutilized tools in methods development are mobile phase pH and elevated temperatures. Hamilton's PRP-C18 column is well-suited for high pH and high temperature applications because the polymer-based stationary phase is chemically inert and has excellent thermal stability above 100 °C.

In modern drug discovery, where analytical HPLC can be a bottleneck, production is streamlined through the use of shorter columns with smaller particles, operated at higher flow rates. The flexibility to employ a high pH mobile phase and elevated temperatures represents further valuable tactics in methods development. These tools, often underutilized or not practical with silica-based columns, enable rapid separation of closely-related basic solutes in their charge-neutral forms that would otherwise co-elute under non-alkaline, ambient temperature conditions.

In this study, 9 structurally-diverse, strongly basic drug compounds are resolved in less than 2 minutes using a high pH mobile phase and a fast acetonitrile gradient at 80 °C.



Fast separation of structurally-diverse, basic solutes at 80 °C

Column:	Hamilton PRP-C18, 5 µm, 2.1 x 33 mm
Flow Rate:	1.0 mL/min
Temperature:	80 °C
Injection Volume:	5 µL
Flow Rate:	1.0 mL/min
Mobile Phases:	A) 30 mM diethylamine (pH 11.5) B) Acetonitrile + 30 mM diethylamine
Gradient:	2 to 99% B in 1 minute
Detection:	UV at 254 nm

Analytes

1. Ephedrine	6. Doxylamine
2. Norephedrine	7. Diphenhydramine
3. Nicotine	8. Nortriptyline
4. Metoprolol	9. Amitriptyline
5. Quinine	

For more information on Hamilton HPLC columns and accessories or to order a product, please visit www.hamiltoncompany.com or call (800) 648-5950 in the US or +41-81-660-60-60 in Europe.

LCGC[®]

north america

MANUSCRIPTS: For manuscript preparation guidelines, see chromatographyonline.com/lcgc-author-guidelines, or call The Editor, (732) 596-0276. LCGC welcomes unsolicited articles, manuscripts, photographs, illustrations, and other materials but cannot be held responsible for their safekeeping or return. Every precaution is taken to ensure accuracy, but LCGC cannot accept responsibility for the accuracy of information supplied herein or for any opinion expressed.

SUBSCRIPTIONS: For subscription and circulation information: LCGC, P.O. Box 457, Cranbury, NJ 08512-0457, or email mmhinfo@mmhgroup.com. Delivery of LCGC outside the United States is 14 days after printing. (LCGC Europe and LCGC Asia Pacific are available free of charge to users and specifiers of chromatographic equipment in Western Europe and Asia and Australia, respectively.)

CHANGE OF ADDRESS: Send change of address to LCGC, P.O. Box 457, Cranbury, NJ 08512-0457; alternately, send change via e-mail to fulfill@mjhassoc.com or go to the following URL: <http://mmhpubs.mmhgroup.com/Welcom.aspx?pubid=LCGC> Allow four to six weeks for change. **PUBLICATIONS MAIL AGREEMENT** No. 40612608. Return all undeliverable Canadian addresses to: IMEX Global Solutions, P.O. Box 25542, London, ON, N6C 6B2, CANADA. Canadian GST number: R-124213133RT001.

C.A.S.T. DATA AND LIST INFORMATION: Contact Melissa Stillwell, tel. (218) 740-6831, e-mail MStillwell@mmhgroup.com.

REPRINTS: Contact Michael J. Tessalone, e-mail: MTessalone@mjhlifesciences.com

INTERNATIONAL LICENSING: Contact Kim Scaffidi, e-mail: kscaffidi@mjhassoc.com

CUSTOMER INQUIRIES: Customer inquiries can be forwarded directly to MJH Life Sciences, Attn: Subscriptions, 2 Clarke Drive, Suite 100, Cranbury, NJ 08512; e-mail: mmhinfo@mmhgroup.com



© 2020 MultiMedia Pharma Sciences, LLC. All rights reserved. No part of this publication may be reproduced or transmitted in any form or by any means, electronic or mechanical including by photocopy, recording, or information storage and retrieval without permission in writing from the publisher. Authorization to photocopy items for internal/educational or personal use, or the internal/educational or personal use of specific clients is granted by MultiMedia Pharma Sciences, LLC. for libraries and other users registered with the Copyright Clearance Center, 222 Rosewood Dr., Danvers, MA 01923, (978) 750-8400, fax (978) 646-8700, or visit <http://www.copyright.com> online. For uses beyond those listed above, please direct your written request to Permission Dept. email: ARockenstein@mjhlifesciences.com

MultiMedia Pharma Sciences, LLC. provides certain customer contact data (such as customer's name, addresses, phone numbers, and e-mail addresses) to third parties who wish to promote relevant products, services, and other opportunities that may be of interest to you. If you do not want MultiMedia Pharma Sciences, LLC. to make your contact information available to third parties for marketing purposes, simply email mmhinfo@mmhgroup.com and a customer service representative will assist you in removing your name from MultiMedia Pharma Sciences, LLC. lists.

LCGC North America does not verify any claims or other information appearing in any of the advertisements contained in the publication, and cannot take responsibility for any losses or other damages incurred by readers in reliance of such content.

To subscribe, email mmhinfo@mmhgroup.com.

485F US Highway One South,
Suite 210
Iselin, NJ 08830
(732) 596-0276
Fax: (732) 647-1235

PUBLISHING/SALES

Senior Vice President, Industry Sciences

Michael J. Tessalone
MTessalone@mjhlifesciences.com

Associate Publisher

Edward Fantuzzi
EFantuzzi@mjhlifesciences.com

Sales Manager

Brianne Molnar
BMolnar@mjhlifesciences.com

Senior Director, Digital Media

Michael Kushner
MKushner@mjhlifesciences.com

EDITORIAL

Editorial Director

Laura Bush
LBush@mjhlifesciences.com

Managing Editor

John Chasse
JChasse@mjhlifesciences.com

Senior Technical Editor

Jerome Workman
JWorkman@mjhlifesciences.com

Associate Editor

Cindy Delonas
CDelonas@mjhlifesciences.com

Creative Director, Publishing

Melissa Feinen
mfeinen@mdmag.com

Senior Art Director

Gwendolyn Salas
gsalas@mjhlifesciences.com

Graphic Designer

Courtney Soden
csoden@mjhlifesciences.com

CONTENT MARKETING

Custom Content Writer

Allissa Marrapodi
AMarrapodi@mjhlifesciences.com

Webcast Operations Manager

Kristen Moore
KMoore@mjhlifesciences.com

Project Manager

Vania Oliveira
VOliveira@mmhgroup.com

Digital Production Manager

Sabina Advani
SAdvani@mjhlifesciences.com

Managing Editor, Special Projects

Kaylynn Chiarello-Ebner
KEbner@mjhlifesciences.com

MARKETING/OPERATIONS

Marketing Manager

Brianne Pangaro
BPangaro@mjhlifesciences.com

C.A.S.T. Data and List Information

Melissa Stillwell
MStillwell@mmhgroup.com

Reprints

Alexandra Rockenstein
ARockenstein@mjhlifesciences.com

Audience Development Manager

Jessica Stariha
JStariha@mmhgroup.com

CORPORATE

Chairman & Founder

Mike Hennessy Sr

Vice Chairman

Jack Lepping

President & CEO

Mike Hennessy Jr

Chief Financial Officer

Neil Glasser, CPA/CFE

Executive Vice President, Global Medical Affairs & Corporate Development

Joe Petroziello

Executive Vice President, Operations

Tom Tolvé

Senior Vice President, Content

Silas Inman

Senior Vice President, I.T. & Enterprise Systems

John Moricone

Senior Vice President, Audience Generation & Product Fulfillment

Joy Puzzo

Vice President, Human Resources & Administration

Shari Lundenberg

Vice President, Business Intelligence

Chris Hennessy

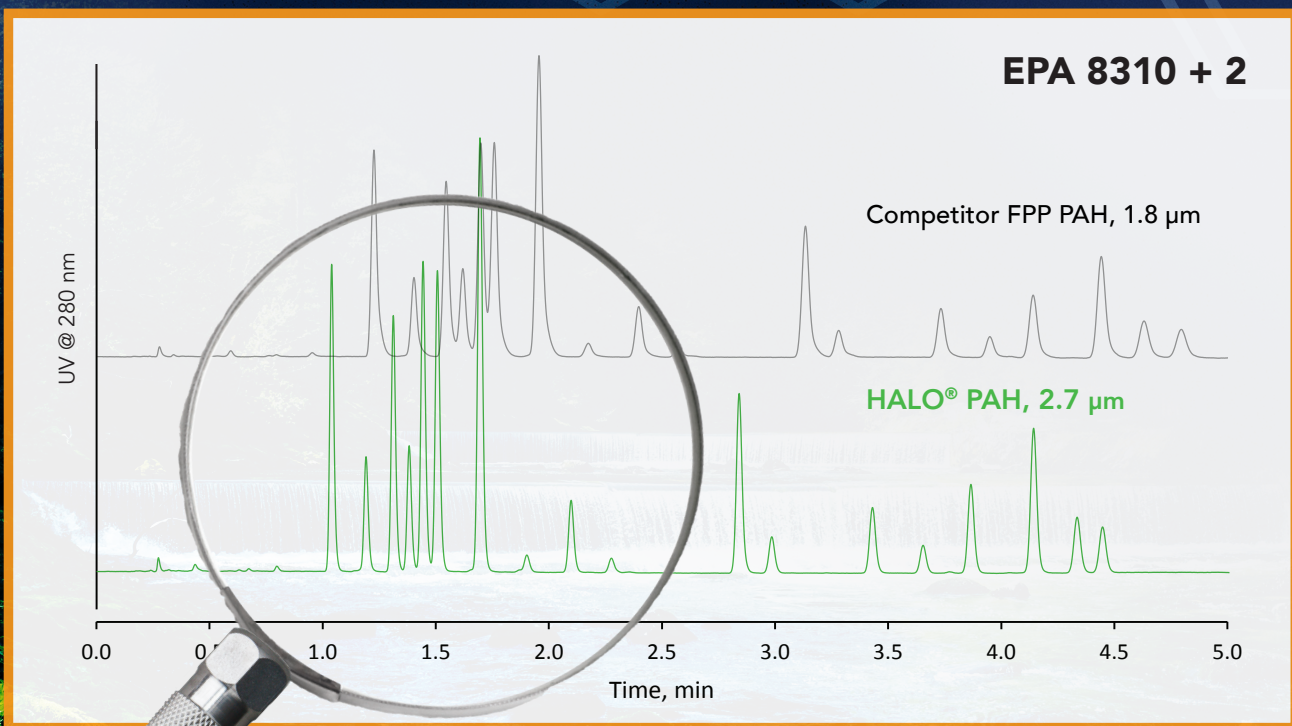
Executive Creative Director, Creative Services

Jeff Brown

HALO®

DISCOVER MORE WITH THE NEW HALO® PAH

Built upon the original and proven Fused-Core® particle technology, the new HALO® PAH outperforms the leading <2 µm fully porous particles (FPP) for high selectivity, higher resolution, and ultra-rugged environmental PAH separations!



DISCOVER MORE!

HALO® and Fused-Core® are registered trademarks of Advanced Materials Technology.

INNOVATION YOU CAN TRUST – PERFORMANCE YOU CAN RELY ON

Recent Developments in LC Column Technology

A supplement to LCGC North America

June 2020

Articles

From Our Guest Editor 7

David Bell

An introduction to this special issue by our guest editor.

Challenges in Obtaining Relevant Information from One- and Two-Dimensional LC Experiments. . . . 8

B.W.J. Pirok and J.A. Westerhuis

To address the quest for greater separation power, the chromatographic community developed comprehensive two-dimensional liquid chromatography (LCxLC). But even with LCxLC, it can still be challenging to analyze highly complex samples and obtain accurate and correct information. In this article, opportunities for optimizing methods for extracting maximum information from one-dimensional (1D)-LC and two-dimensional (2D)-LC chromatographic data are explained.

The Potential for Portable Capillary Liquid Chromatography. . . . 15

James P. Grinias

Is the desired goal of “shrinking down” capillary liquid chromatography (LC) from large laboratory systems to accurate portable field instruments realistic? This article explores recent progress in the miniaturization of LC components—such as capillary LC columns, micro- and nano-flow pumps, detectors, and other essential system components—and the future outlook for operating capillary LC instruments in remote settings.

Biocompatible Microextraction Devices for Simple and Green Analysis of Complex Systems. . . . 25

Emanuela Gionfriddo

Pretreatment of complex samples remains a key step in the analytical workflow, critically impacting the overall accuracy of results. Pretreatment methods have been a challenge for food, biofluids, and environmental samples. Here, the development and evolution of biocompatible solid-phase microextraction (bio-SPME) as a sample pretreatment method are discussed for use in liquid chromatography and direct mass spectrometry applications.

Boosting the Purification Process of Biopharmaceuticals by Means of Continuous Chromatography. . 30

Chiara De Luca, Simona Felletti, Giulio Lievore, Alessandro Buratti, Mattia Sponchioni, Alberto Cavazzini, Martina Catani, Marco Macis, Antonio Ricci, and Walter Cabri

Single-column (batch) chromatography, involving two or more successive single-column (batch) chromatographic steps, is a standard approach for purifying biopharmaceuticals. Step one, known as the capture step, is used to remove product-related impurities, and step two, the polishing step, is used to remove product-related impurities. Here we present and illustrate the advantages of continuous chromatography for these separations: capture simulated moving bed (captureSMB) for the capture step and multicolumn countercurrent solvent gradient purification (MCSGP) for polishing.

From Our Guest Editor

Welcome to the 2020 edition of *Recent Developments in LC Column Technology*. Inspiration for this collection of articles stemmed from some personal observations at recent conferences (though this now seems like the distant past). The main observation was that there is new group of highly talented scientists emerging in the realm of separation science. Upon reflection, I suppose this is not uncommon in most fields of study, and is rather continuous in our own, but the high level of talent from the current group has been remarkable. When asked to put a supplement together on recent developments in LC technology, I wanted to seek out some of these “emerging” scientists and showcase their contributions.

B.W.J. Pirok and J.A. Westerhuis of the University of Amsterdam lead the issue off with a discussion regarding the challenges of extracting relevant information from high-demand, modern chromatographic data.

Recent developments and future perspectives in the quest for portable LC systems is presented by James P. Grinias of Rowan University, in Glassboro, New Jersey.

Emanuela Gionfriddo of The University of Toledo, in Toledo, Ohio, then considers the role of microextraction for the pretreatment of complex samples for LC analysis.

Finally, Martina Catani of the University of Ferrara, in Ferrara, Italy, and her coauthors examine the important topic of biopharmaceutical purification via continuous chromatographic techniques.

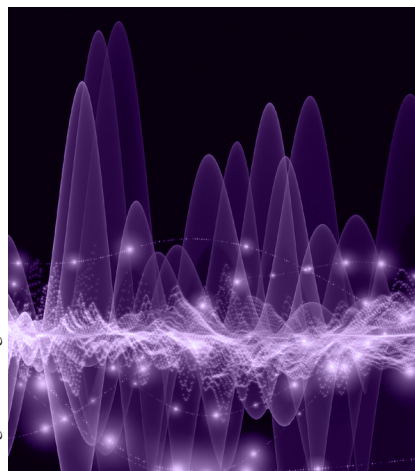
The response to this “emerging scientist” theme was overwhelming. What lies within the following pages is just a sample of the great work this next generation of scientists is producing. More efforts from additional emerging scientists will be published in coming issues of *LCGC North America* and, I hope, future supplements. Enjoy.



David Bell
Director of Research and Development,
Restek Corporation

Challenges in Obtaining Relevant Information from One- and Two-Dimensional LC Experiments

Image credit: agsandrew/stock.adobe.com



Liquid chromatography (LC) methods are continuously improving to maintain our ability to meet the growing need of society to obtain more reliable information about a number of sample characteristics. With the samples subjected to LC analysis becoming increasingly complex, analysis of the resulting convoluted data has been increasingly challenging. To aid identification and quantification, LC systems were hyphenated with multichannel detectors (such as mass spectrometry [MS] and ultraviolet-visible spectroscopy [UV-vis]), which yielded relief to some extent, but also required new advanced data analysis methods. Not waiting for an answer, the chromatographic community resorted to the tool it understood best to address the quest for more separation power, and developed comprehensive two-dimensional (2D) chromatography. However, even with 2D chromatography, it can still be difficult to extract accurate and correct information from the results obtained for highly complex samples. Use of sophisticated detectors, such as high-resolution mass spectrometers, certainly helps, but also generates mountains of data. Arguably, extracting all relevant information is the biggest challenge currently faced in high-resolution chromatography. In this article, the challenge of and opportunities for extracting information from one-dimensional (1D)-LC and 2D-LC data is explained.

The increasing complexity of samples continues to demand more and more from liquid chromatography (LC) methods. To meet the call for better separations, scientists across the chromatographic community have enhanced the overall performance of LC in several ways. Well-known examples include the extremely efficient superficially-porous particles, novel stationary-phase monolithic materials, hardware to support ultrahigh-pressure liquid chromatography (UHPLC) conditions, and elevated temperatures. These approaches are generally aimed to improve the efficiency of the system, thus effectively reducing the peak widths and consequently the likelihood of peak overlap. However, Carr and associates demonstrated that these developments would mainly benefit from fast separations up to a limited number of analytes (1). Despite the use of state-of-the-art separation power, samples comprising of more than 50

analytes were shown to likely yield (partially) co-eluted peaks.

Fortunately for chromatographers, the chemometrics community proceeded to develop algorithms to extract as much accurate information (such as peak area for quantification) as possible from the increasingly more densely populated chromatograms. While we can find many of these algorithms in the data analysis software packages that accompany LC systems, the more convoluted signals become ever more challenging to unravel.

Background Removal

Generally, data analysis workflows start by removing the noise and baseline drift of the signal. In practice, a chromatographer will generally use blank measurements, but this is not always possible, or desired. More importantly, subsequent steps in the data-processing workflow, such as peak detection

**B.W.J. Pirok and
J.A. Westerhuis**

Creating Reproducible and Innovative Separation Solutions Since 1980

Any Scale

YMC supports separations from capillary to process manufacturing.

Anywhere

YMC Group delivers global availability and support.

Any Mode

Phases include reversed phase, normal phase, HIC, HILIC, core-shell, chiral, SEC, and IEX.

Any Format

Bulk supply and columns for capillary LC, Fast LC, UHPLC, HPLC, semi-prep, prep, SMB, SFC.

Any Application

Biomolecules, small molecule APIs, chemicals, natural products, much more.

YMC
AMERICA, INC.

www.ymcamerica.com • info@ymcamerica.com

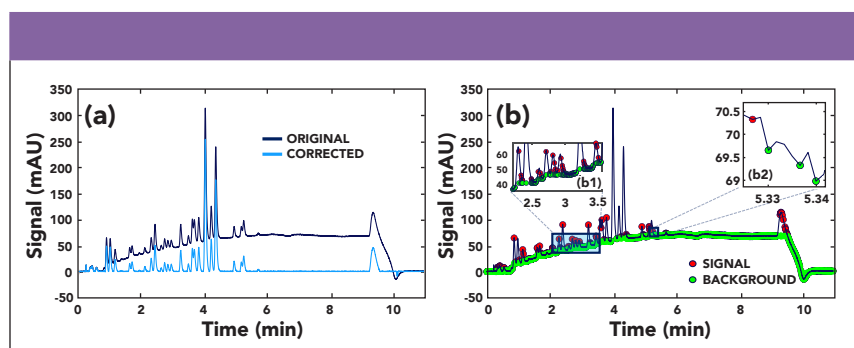


Figure 1: Illustration of background correction by the local minimum value (LMV) approach. (a) Overlay of unprocessed (dark blue) and corrected signal (light blue). (b) The LMV approach searches all datapoints that are of lower value than their neighbors. Local minima on peaks (red) are identified using outlier detection and thresholding, whereas background points (green) are not. Inset (b1): close-up for populated region. Inset (b2): Local minima at the foot of a peak (left points).

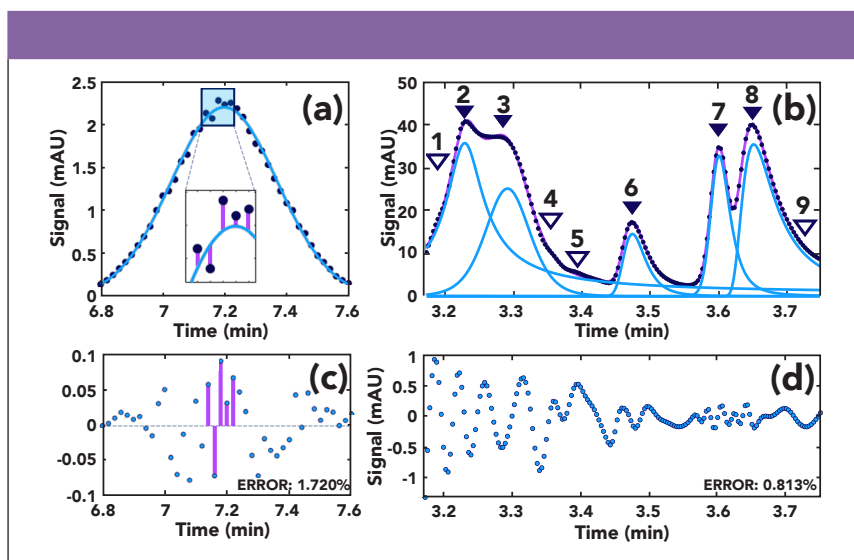


Figure 2: (a) Gaussian fitted (light blue) through data points and the residuals (purple). (b) The presence of undetected peaks (light triangle) disturbs the curve fitting for many detected peaks (dark triangle). (c) and (d) Residual plot for panels (a) and (b), respectively.

or multivariate methods, often rely on removing the background beyond that which can be achieved by simply subtracting a blank. Looking at just the last decade, this need for background removal has spurred the development of univariate and multivariate algorithms with more than 15 different methods (2).

The rationale for this astounding number of approaches can be found in three characteristics. First, “background” is an umbrella term for a large variation of different phenomena, ranging from simple baseline drift to the occurrence of complex systems peaks, and different phenomena require different solutions; second, successful background removal equals preventing accidental removal of sample-related information;

and third, the more sophisticated algorithms must be tailored to the characteristics of the dataset. In practice, the latter means that the user or algorithm must first determine optimal parameters for operation.

An example of a method to remove background is the local minimum value (LMV) approach (3). In Figure 1a, unprocessed data can be seen to contain the baseline drift resulting from the use of gradient elution. Figure 1b clarifies how the LMV approach literally searches all local minima of the signal (such as points that feature a lower signal than neighboring points; see Inset, Figure 2b). Using a moving-window approach and thresholding, outliers are identified along the chromatogram. Local minima on peaks

or their edges (red points) can therefore be distinguished from the background (green points). Understandably, this and other strategies rely on the availability of data points that describe the background (3–5), thus becoming weaker when chromatograms are less sparsely populated and potentially preserving system peaks. Alternative approaches exist to tackle these limitations, but, despite their elegance (6), generally require more user input to work effectively in particular when more co-elution occurs. Unfortunately, numerical data comparing the vast number of strategies is limited (2).

Peak Detection and Analysis

Having removed the background, we can now shift our attention to the information of interest: the actual peaks. Traditionally, approaches for peak detection generally use either the derivatives of the signal, or curve-fitting strategies (7). Methods utilizing the derivatives exploit the fact that the peak apex as well as peak start and end points can be detected using the first- and second-order derivative of the signal, respectively. This strategy effectively amplifies the variation in the signal. To avoid local maxima (as present in noise) being recognized as peaks, derivative-based approaches generally rely on thorough removal of the background at the risk of removing sample information, potentially resulting in false negatives (for example, undetected components at trace concentrations) (8,9). Moreover, the use of derivatives becomes rather challenging when peaks are insufficiently resolved.

While this is also true for curve-fitting strategies, such matched-filter response approaches are arguably more forgiving. These least-squares methods attempt to fit a distribution function (such as a Gaussian) to the signal (10,11). To understand this, we remember that a Gaussian distribution can be expressed as

$$f(x) = \frac{1}{\sigma\sqrt{\pi}} e^{-\frac{1}{2}\left(\frac{x-\mu}{\sigma}\right)^2} \quad [1]$$

where σ is the standard deviation of the distribution and μ the mean. The curve-fit process essentially involves finding σ and μ values such that the residuals, the difference between the modeled Gaussian and the true signal (the error), are minimized. This approach typically utilizes optimization algorithms to iteratively update σ and μ , until the

error is minimal. This is illustrated in Figure 2a, where the resulting Gaussian model (light blue) can be seen to match the data points. The residuals (purple lines) are plotted in Figure 2c, representing a total error of 1.72%.

Curve fitting is an elegant approach that, in contrast to derivative-based methods, does not necessarily require extensive preprocessing of the data (8). While we will see further how curve fitting can offer refuge in the event of co-eluted peaks, Figure 2b shows that this is limited when co-elution is too severe. Several peaks are undetected (light triangles) resulting in distorted fits of the actual detected peaks (dark triangles with individual light-blue curves). While the error is merely 0.813%, the wave patterns in the residual plot (Figure 2d) do note the deviation. Another piece of evidence can be found in the vastly different peak widths for the detected peaks (Figure 2b, light blue lines). It should be noted that both derivative-based and curve-fitting approaches struggle to detect peaks that are not prominently visible in Figure 2b. Indeed, the prominence of these peaks (the measure of how much a peak stands out due to its intrinsic height and location relative to neighboring peaks) is rather limited.

For peak detection by this approach to work in the event of severe co-elution, the strategy requires information on the number of peaks present, which ultimately is a peak detection problem. Ironically, to tackle this, curve-fitting approaches often exploit derivative-based methods to guide the least-squares process by offering the number of expected peaks and best guesses for the distribution functions. For example, if the curve-fit process is equipped with the suspected location of a peak, then this can be used as initial guess of the μ parameter of the distribution function, thus increasing the likelihood of successful deconvolution is increased.

Deconvolution to Facilitate Quantification

Ultimately, the peak detection serves to subsequently obtain all relevant information from that peak. This, of course, includes the determination of the area to allow quantification. Figure 3a shows the detection and integration of peaks as commonly encountered in data-analysis software for LC instruments. Indeed, the way peaks 2 and 3 are divided (purple line) does not appear

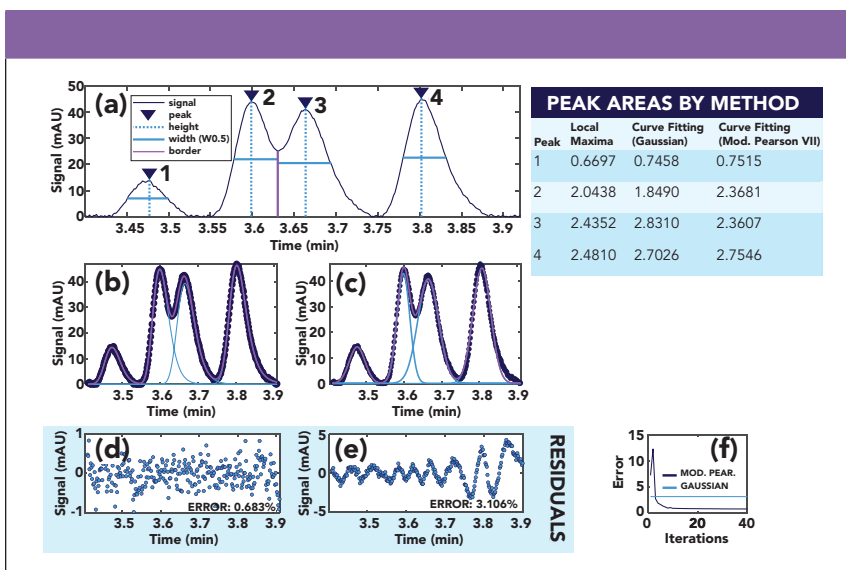


Figure 3: The choice of strategy can have a significant impact on the obtained peak areas. (a) Rough assessment of peaks through local maxima. The purple line depicts the end of peak 2 and start of peak 3 according to this method. (b) and (c) Curve fitting results for the same signal using a modified Pearson VII (12) (b) and Gaussian (c) distribution function, with the corresponding residuals in panels (d) and (e), respectively. (f) Number of iterations to arrive at obtained fits for Gaussian (light blue) and modified Pearson VII (dark blue) distributions. The inset table lists the different peak areas obtained for the different methods.

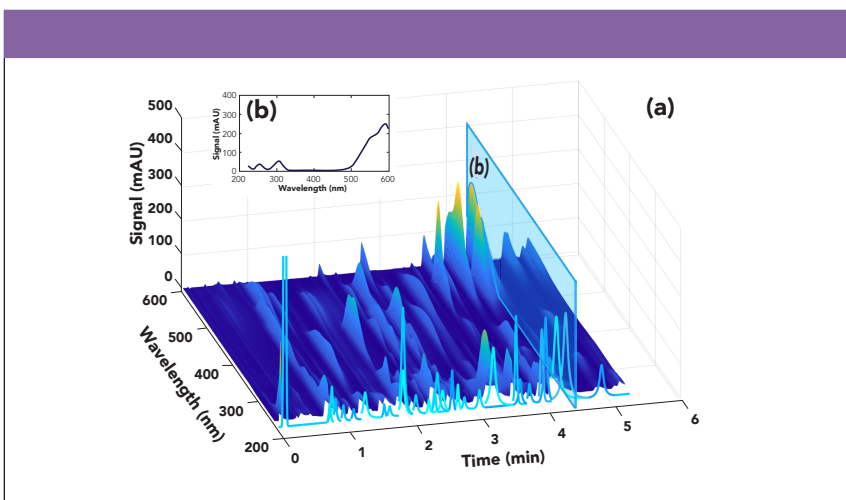


Figure 4: (a) 3D plot of LC-DAD data with, on the foreground, the individual elution profiles of all detected analytes as determined by MCR-ALS. (b) Example of UV-vis spectrum. The availability of the additional detector dimension facilitates computationally resolving co-eluted compounds.

very accurate, because the actual shape of the peak is no longer preserved. Curve fitting appears to be an excellent method to tackle this problem. However, peaks in LC tend to tail slightly, even in the best separations. Consequently, it is of paramount importance that our distribution function can describe this asymmetric shape. In contrast to the symmetric Gaussian, the modified Pearson VII distribution represents the

typical shape of a peak in LC rather well (12). It is expressed as:

$$f(x) = \left(1 + \frac{(x - \mu)^2}{M(\sigma + E(x - \mu))^2}\right)^{-M} \quad [2]$$

where the additional parameter E represents the asymmetry of the peak, while M represents the shape, defined somewhere in between a modified Lorentzian ($M = 1$) and

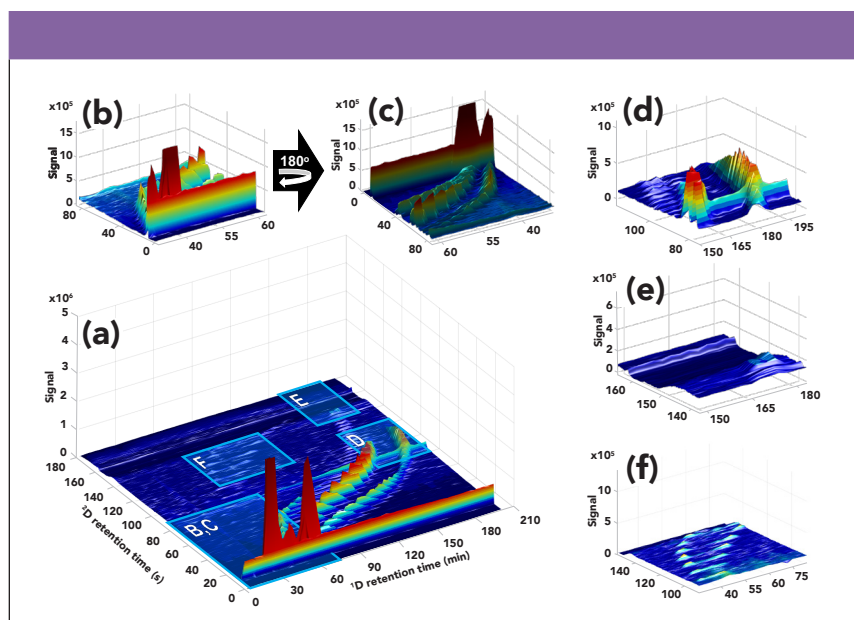


Figure 5: Depiction of the complex background signal in LC \times LC separations. (a) Separation of an industrial surfactant sample by LC \times LC with charged aerosol detection. (b) The variation in mobile-phase components in 1D effluent may yield systematic signals in the 2D , which requires (c) different data preprocessing than the background signals frequently encountered in the vicinity of regular peaks. (d) Effects such as 1D column bleed and injection effects may cause unwanted system phenomena that have to be removed. (e) 2D gradients cause background distortions. For state-of-the-art methods, these vary as a function of time if shifting gradients are employed. (f) As peaks increasingly co-elute, the limited sampling of the 1D effluent complicates peak detection.

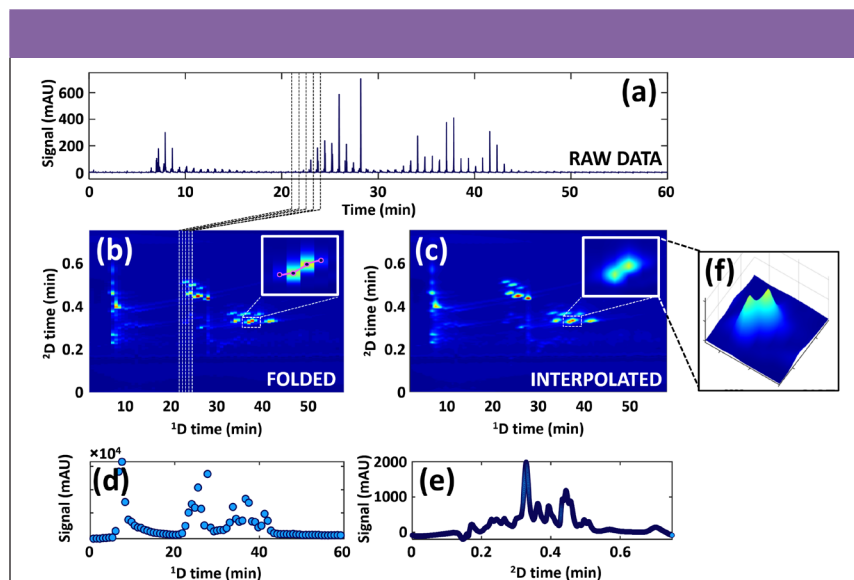


Figure 6: (a) Example of a raw LC \times LC chromatogram. Dashed lines depict 2D modulations. (b) Folded 2D plot of raw data shown in panel (a). (c) Interpolated version of data shown in panel (b). (d) 1D chromatogram by summing all 2D datapoints. (e) 2D chromatogram by summing all 1D datapoints. (f) Small shifts in retention time can result in the detection of two peaks.

a Gaussian ($M = \infty$) shape. (13). Good estimate values for E and M are 0.15 and 5 (12).

The flexibility of equation 2 to adapt itself to the actual shape of the peak is expressed in Figure 3b, where the distribution function can be seen to accurately describe all four elu-

tion bands. In contrast, the Gaussian distribution cannot accommodate the asymmetric shape of LC peaks as accurately for this data (Figure 3c). These observations are supported by the residual plots in Figures 3d and 3e for the modified Pearson VII and Gaussian dis-

tribution, respectively. Indeed, in Figure 3d, the residuals appear to be randomly distributed as noise, whereas the pattern in Figure 3e reveals the misrepresentation of sections of the signal. Figure 3f shows that, after a limited number of iterations (<10), good fits can be obtained, representing a computation time of a few seconds.

More importantly, however, are the peak areas listed in Figure 3. The found area for peaks 2 and 3 using the local-maxima approach (Figure 3a) note 2.04 and 2.44, respectively. Using the modified Pearson VII as distribution function to accurately describe the peak shape, we obtain 2.37 and 2.36 using the curve-fitting approach (Figure 3b). This is a significant difference and indicates the importance of accurate deconvolution of peaks. However, a look at the numbers of 1.85 and 2.83 for peaks 2 and 3, respectively, as obtained using a Gaussian distribution function (Figure 3c), also underlines the magnitude to which curve-fitting approaches rely on the finding a representative distribution function. This threat adds to the questionable performance when even more peaks are co-eluted. Ultimately, non-random residuals are an important indicator for incorrect selection of peak shape and number of peaks.

At this point, it is relevant to note that, in contrast to the time domain, deconvolution is also possible in the frequency domain of the signal. While indispensable in data processing of spectroscopic data (7), it has also been extensively applied to chromatographic data (14), including two-dimensional data (15). Examples include the study of band broadening (16,17), but it is also applied for resolution enhancement (7). A recent example of the power of the latter is the work by Hellinghausen and associates (18). The work is a good example of how chemometric methods may yield additional “virtual” peak capacity without increasing the analysis time.

Returning to our time-domain deconvolution, one intrinsic problem with both the derivative-based and curve-fitting based methods is that they are designed to provide a binary answer to the questions of whether a signal is a peak or not. We have seen that this inevitably yields false negatives, and that information is lost. In this context, one interesting alternative peak-detection technique is therefore the probabilistic method by Lopatka and coworkers, which employs a Bayesian inferential approach (19). In essence, this approach exploits the statistical-overlap

theory as prior information of existence of a peak. The algorithm postulates an array of exclusive hypotheses covering whether a peak is present or not, and evaluates these using least-squares. This strategy does not rely on the height of the peak, and should deserve additional attention.

Multichannel Data

Of course, chromatographers had a different solution to the problem of peaks co-elution. By hyphenating the LC with more sophisticated detection techniques such as diode-array detection (DAD), the powerful mass spectrometer yields more information to distinguish co-eluted peaks. Until now, we have addressed data analysis for data where only one property or variable is measured as a function of time, commonly referred to as *first-order* or *single channel* data. Using a DAD or MS detector, we measure an array of variables simultaneously, obtaining *multichannel* or *second-order* data. While data-analysis strategies in some cases approach these data from a single-channel perspective, such as the total ion-current chromatogram (TIC) or extracted-ion chromatogram (XIC), exploiting the multichannel content is often worth the investment. Multichannel data offer additional information to achieve more powerful deconvolution using multivariate methods. An example is multivariate curve resolution asymmetric least squares (MCR-ALS), which is applied to the dataset shown in Figure 4 to provide elution profiles and analyte spectra for all analytes detected.

In Figure 4a, we see the absorption for a range of wavelengths as a function of time plotted in a 3D surface, and can immediately understand that it is easier to spot differences between neighboring eluted species. For every point in time a UV-vis spectrum is obtained (Figure 4b). This is exploited by the MCR-ALS strategy, and the obtained individual elution profiles are plotted in the foreground for each compound. The approach not only allows resolving elution profiles of neighboring peaks, but also their corresponding UV-vis spectra. Similarly, multivariate data analysis methods for background correction have also been developed (20,21).

The information density in the detector dimension is arguably even higher for LC-MS data. When we trade the linear response of UV-vis for the resolution offered by MS,

our dataset contains much more information and is considerably larger. This is particularly true when high-resolution MS instruments are employed. Even in cases of severe co-elution, it is often possible to find compounds present at trace concentrations using LC-MS.

Although multivariate methods are potentially more powerful to detect analytes in multichannel data, they are not yet commonly used by the chromatographic community. They are more difficult to automate (often needing prior information and parameter setting), and are, therefore, also less frequently supported in software packages accompanying the instrumentation. More experience and more interaction between developers and practitioners is needed for these methods to reach their full potential.

Comprehensive Two-dimensional LC

Chromatographers have responded with a familiar solution by adding a second separation dimension to their LC. Comprehensive two-dimensional liquid chromatography (LC \times LC), where all fractions of first-dimension (1 D) effluent are subjected to a second-dimension (2 D) separation, certainly has delivered the much needed additional resolving power (22).

Unfortunately, while the added separation power may aid in reducing the likelihood of co-elution, it does not aid in extracting the key characteristics of the peaks. In contrast, particularly when multichannel detectors are used, higher-order data require innovative approaches.

That analysis of LC \times LC data is more challenging is illustrated in Figure 5. The chromatogram in Figure 5a comprises a separation of an industrial surfactant sample (23). A background correction for such separations is not straightforward. For example, the characteristic elution of unretained species, resulting in a large signal, now results in a ridge across the entire chromatogram (Figure 5b). This ridge may shroud unretained analytes and is likely to change as the 1 D gradient alters the 1 D column effluent. Such phenomena require significantly different preprocessing strategies than the background encountered in the vicinity of resolved analytes (Figure 5c). At the same time, effects such as 1 D column bleed, injection effects, as well as incompatible species introduced into the 2 D separation may cause system phenomena which must be removed (Figure 5d).

Generally, LC \times LC methods employ gradient elution in the second dimension to facilitate rapid elution and reduce the modulation time. The background signal induced by the gradient (Figure 5e) now must be removed from the entire 2D chromatogram. However, shifting gradients, which allows the 2 D gradient to be changed for each individual modulation as a function of time (24), the background will be expressed differently for each modulation. Finally, the 1 D is often sampled minimally to facilitate shorter analysis times (24). As a rule of thumb, 1 D peaks are sampled three to four times by the 2 D, significantly reducing the data available to describe the 1D peak shape. When this undersampling results in the loss of the ability to distinguish neighboring peaks, peak detection, integration, and thus quantification becomes challenging (Figure 5f).

To understand the cause, we must revisit the origin of the data. In LC \times LC, the detector continuously measures the 2 D effluent, resulting in a very long one-dimensional chromatogram (Figure 6a) which comprises a series of 2 D chromatograms. Using the modulation time, the 1D chromatogram can be divided to obtain the individual 2 D separations, which can be stacked next to each other. This process, typically referred to as folding the chromatogram, is highlighted in Figure 5b, with the dashed lines representing the individual 2 D separations or *modulations*.

The chromatogram shown in Figure 6b is arguably difficult to interpret with the pixelated 1 D information. With the 1 D sampling rate depending entirely on the modulation time, Figure 6d strikingly underlines the shortage of data in the 1 D. This is in stark contrast to the surplus of data in the 2 D (Figure 6e). To achieve a smoother 1 D profile and facilitate further data processing, the signal is often interpolated (25) resulting in the chromatogram as shown in Figure 6c.

The two most popular approaches for peak detection in 2D separations are the two-step and the watershed approach. The two-step approach first performs peak detection on the 1D data for each 2 D chromatogram according to the derivative-based approach as discussed previously (26). Relevant peak characteristics are obtained through computation of the statistical moments. Next, a clustering algorithm is used to merge the signals in neighboring modulations which belong to the same chromatographic 2D peak (see Inset, Figure 6b). In contrast, the inverted

watershed approach exploits the topology of the 2D surface to define the boundaries of the 2D peak (27).

Where the two-step algorithm is vulnerable to erroneous clustering in the event of severe co-elution, the watershed algorithm has been shown to be vulnerable to preprocessing and incorrect peak alignment (28). Both algorithms have since seen significant development, with improved peak alignment for the watershed algorithm (29) and a Bayesian two-step approach to benefit from multichannel detectors in four-way data (30). The magnitude of the peak-detection challenge is shown in Figure 6f. This 3D view of the inset of Figure 6c shows how interpolation may suggest the presence of two peaks, whereas the normal data (Inset, Figure 6b) also leave room for the signal to represent just one peak. With modern LC×LC methods employing shifting gradients and extremely fast 2D gradients (22), small shifts in retention across multiple modulations are not uncommon and can be different for each 2D peak within an LC×LC separation. This is also visible in Figure 6b, and suggests that method-wide retention time alignment may be insufficient to resolve this issue.

In these complex cases, the addition of multichannel detectors (such as LC×LC-MS and LC×LC-DAD) is the key to discern the true elution profiles of peaks. Two examples of multivariate techniques that are employed to tackle these complex higher-order datasets are MCR-ALS and parallel-factor analysis 2 (PARAFAC2) (31,32). Both techniques have been applied to LC×LC utilizing DAD and MS data and have shown to be highly useful (33–37). However, as with their application to 1D-LC data, these methods are currently still vulnerable for insufficient background correction and not straightforward to use. Often their application requires tailoring the algorithm with optimal parameters and constraints to the dataset. In this context, the development of PARAFAC2-based deconvolution and identification system (PARADISE) framework for gas chromatography–mass spectrometry (38) and LC–MS (32) is particularly interesting. This freely available platform was specifically designed to offer the power of PARAFAC2 to analyze chromatographic data with minimal user-defined settings. Similarly, toolboxes have been developed for MCR-ALS (39).

Multidimensional data-analysis techniques allow complex higher-order data generated by state-of-the-art (LC×)LC–MS and (LC×)LC–DAD methods to be unraveled. Their development may deliver increased information without increasing the analysis time. These techniques certainly deserve the attention from the chromatographic community, yet currently there appears to be a gap between development of such methods and large-scale use.

Acknowledgments

B.W.J. Pirok acknowledges the Agilent University Relations grant #4354 for support and Denice van Herwerden for her assistance with Figure 4.

References

- (1) P. W. Carr, X. Wang, and D. R. Stoll, *Anal. Chem.* **81**(13), 5342–5353 (2009).
- (2) T. S. Bos et al., *J. Sep. Sci.* submitted (2020).
- (3) H.Y. Fu et al., *J. Chromatogr. A* **1449**, 89–99 (2016).
- (4) X. Ning, I.W. Selesnick, and L. Duval, *Chemom. Intell. Lab. Syst.* **139**, 156–167 (2014).
- (5) P.H.C. Eilers and H.F.M. Boelens, *Life Sci.* (2005). doi:10.1021/ac034173t
- (6) M. Lopatka, A. Barcaru, M. Sjerps, and G. Vivó-Truyols, *J. Chromatogr. A* **1431**, 122–130 (2016).
- (7) A. Felinger, *Data Analysis and Signal Processing in Chromatography* (Elsevier Science Publishers B.V., Amsterdam, The Netherlands, 1998).
- (8) K.M. Pierce and R.E. Mohler, *Sep. Purif. Rev.* **41**(2), 143–168 (2012).
- (9) R. Danielsson, D. Bylund, and K.E. Markides, *Anal. Chim. Acta* **454**(2), 167–184 (2002).
- (10) B. van den Bogaert, H.F.M. Boelens, and H.C. Smit, *Anal. Chim. Acta* **274**(1), 87–97 (1993).
- (11) J. Beens, H. Boelens, R. Tijssen, and J. Blomberg, *J. High Resolut. Chromatogr.* **21**(1), 47–54 (1998).
- (12) B.W.J. Pirok et al., *Anal. Chim. Acta* **1054**, 184–192 (2019).
- (13) G.R. McGowan and M.A. Langhorst, *J. Colloid Interface Sci.* **89**(1), 94–106 (1982).
- (14) A. Felinger, *Anal. Chem.* **66**(19), 3066–3072 (1994).
- (15) A.T. Hanke et al., *J. Chromatogr. A* **1394**, 54–61 (2015).
- (16) Y. Vanderheyden, K. Broeckhoven, and G. Desmet, *J. Chromatogr. A* **1465**, 126–142 (2016).
- (17) N.A. Wright, D.C. Villalanti, and M.F. Burke, *Anal. Chem.* **54**(11), 1735–1738 (1982).
- (18) G. Hellinghausen, M.F. Wahab, and D.W. Armstrong, *Anal. Bioanal. Chem.* **412**(8), 1925–1932 (2020).
- (19) M. Lopatka, G. Vivó-Truyols, and M.J. Sjerps,

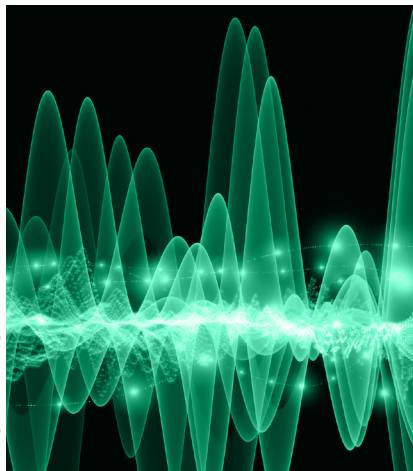
Anal. Chim. Acta **817**, 9–16 (2014).

- (20) H.F.M. Boelens, R.J. Dijkstra, P.H.C. Eilers, F. Fitzpatrick, and J.A. Westerhuis, *J. Chromatogr. A* **1057**(1–2), 21–30 (2004).
- (21) J. Peng et al., *Anal. Chim. Acta* **683**(1), 63–68 (2010).
- (22) B.W.J. Pirok, D.R. Stoll, and P.J. Schoenmakers, *Anal. Chem.* **91**(1), 240–263 (2019).
- (23) B.W.J. Pirok, T.H. Halmans, R. Edam, and A.A. van Heuzen, *Shell Global Solutions*, unpublished (2015).
- (24) B.W.J. Pirok, A.F.G. Gargano, and P. J. Schoenmakers, *J. Sep. Sci.* **41**(1), 68–98 (2018).
- (25) R.C. Allen and S.C. Rutan, *Anal. Chim. Acta* **705**(1–2), 253–260 (2011).
- (26) S. Peters, G. Vivó-Truyols, P.J. Marriott, and P.J. Schoenmakers, *J. Chromatogr. A* **1156**(1–2), 14–24 (2007).
- (27) S.E. Reichenbach, M. Ni, V. Kottapalli, and A. Visvanathan, *Chemom. Intell. Lab. Syst.* **71**(2), 107–120 (2004).
- (28) G. Vivó-Truyols and H.-G. Janssen, *J. Chromatogr. A* **1217**(8), 1375–1385 (2010).
- (29) I. Latha, S.E. Reichenbach, and Q. Tao, *J. Chromatogr. A* **1218**(38), 6792–6798 (2011).
- (30) G. Vivó-Truyols, *Anal. Chem.* **84**(6), 2622–2630 (2012).
- (31) R. Bro, *Chemom. Intell. Lab. Syst.* **38**(2), 149–171 (1997).
- (32) B. Khakimov, J.M. Amigo, S. Bak, and S. B. Engelsen, *J. Chromatogr. A* **1266**, 84–94 (2012).
- (33) S.E.G. Porter, D.R. Stoll, S.C. Rutan, P.W. Carr, and J.D. Cohen, *Anal. Chem.* **78**(15), 5559–5569 (2006).
- (34) M. Navarro-Reig, J. Jaumot, T.A. van Beek, G. Vivó-Truyols, and R. Tauler, *Talanta* **160**, 624–635 (2016).
- (35) M. Navarro-Reig et al., *Anal. Chem.* **89**(14), 7675–7683 (2017).
- (36) D.W. Cook, S.C. Rutan, D.R. Stoll, and P.W. Carr, *Anal. Chim. Acta* **859**, 87–95 (2015).
- (37) R.C. Allen and S.C. Rutan, *Anal. Chim. Acta* **723**, 7–17 (2012).
- (38) A.B. Risum and R. Bro, *Talanta* **204**, 255–260 (2019).
- (39) R. Tauler, A. de Juan, and J. Jaumot, MCR-ALS Toolbox at <http://www.mcrals.info/>

B.W.J. Pirok is an assistant professor with the Analytical Chemistry Group, van 't Hoff Institute for Molecular Sciences, Faculty of Science, at the University of Amsterdam, in The Netherlands. **J.A. Westerhuis** is with the Faculty of Science at the Swammerdam Institute for Life Sciences, at the University of Amsterdam, in The Netherlands. Direct correspondence to: B.W.J.Pirok@uva.nl

The Potential for Portable Capillary Liquid Chromatography

Image credit: agsandrew/stock.adobe.com



Liquid chromatography (LC) is one of the most widely used analytical techniques in the world. However, unlike many other chemical measurement technologies, it has not been “miniaturized” to the same extent. Over the past several years, a number of developments related to the preparation of columns on the capillary scale and the design of portable instrument components have made the goal of “shrinking down” LC more realistic. New approaches to the design of capillary LC columns, including improved packing strategies in fused silica tubular formats and the manufacture of microfabricated pillar array columns, have led to major advances in chromatographic performance. Micro- and nano-flow pumps, detectors, and other system components have been scaled down to be more compatible with these columns, while also creating the opportunity to operate instruments in remote settings. This recent progress in capillary LC, and the future outlook of the field, are discussed here.

Research in the area of capillary liquid chromatography (LC) has endured for more than 40 years (1). I began working in this area in the fall of 2009, when I joined the University of North Carolina at Chapel Hill as a graduate student under the direction of Professor James Jorgenson. It was around this time that he published an in-depth review on the topic of capillary ultrahigh-pressure liquid chromatography (UHPLC) (2), a technique his research group established in the late 1990s and early 2000s (3–7). Since that article was published, new approaches to studying the design and performance of capillary LC columns were demonstrated, and significant progress in the design of miniaturized LC instrument components was made. My colleagues and I have recently discussed various aspects of capillary LC, both here in LC–GC (8,9) and elsewhere (10,11). The goal of this article is to provide an assessment of the implications of these developments on the future of portable capillary LC instrumentation.

James P. Grinias

Capillary LC Column Design

In recent years, fundamental investigations have helped improve our understanding of capillary LC column preparation (12–14). In 2010, the Tallarek group of Philipps-Universität Marburg demonstrated the ability to image the inside of capillary LC columns by utilizing confocal laser scanning microscopy (CLSM), from which a computational reconstruction of the bed structure could be generated and used to measure the column's physical characteristics (15,16). Originally demonstrated for the characterization of monolithic stationary phase structures, the strategy was adapted to particle-packed beds as well (17). These original reports focused on bare silica, but an adapted technique using a hydrophobic fluorescent dye for the CLSM imaging process soon enabled the ability to image capillary columns packed with reversed-phase particles (Figure 1a) (18). This allowed for the first direct correlation between observed column efficiency and the morphology of the packed bed, providing new insight into the structural characteristics that influence chromatographic band broadening. Results showed that radial homogeneity of the packed bed plays a key

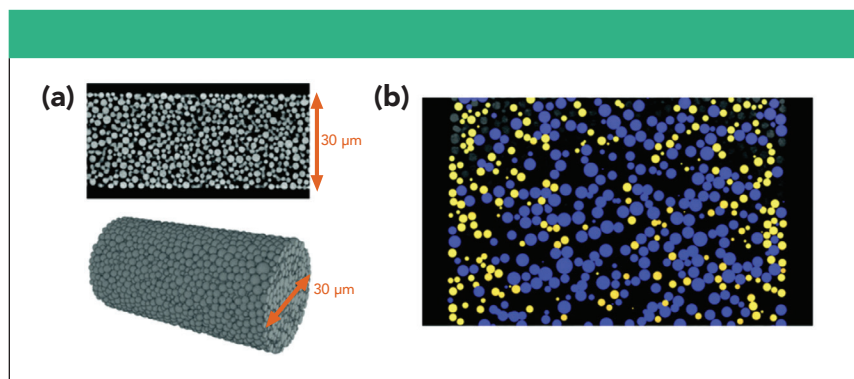


Figure 1: In panel (a), a single CLSM image of a 30- μm i.d. capillary column packed with 1.9- μm particles and a full computational reconstruction of bed morphology derived from many of these images scanned axially through the capillary are shown. In panel (b), size segregation effects in a 75- μm i.d. capillary column packed with 1.9- μm particles in which smaller particles (in yellow) are concentrated at the column walls and larger particles (in blue) populate the bulk packing region. Adapted with permission from (18).

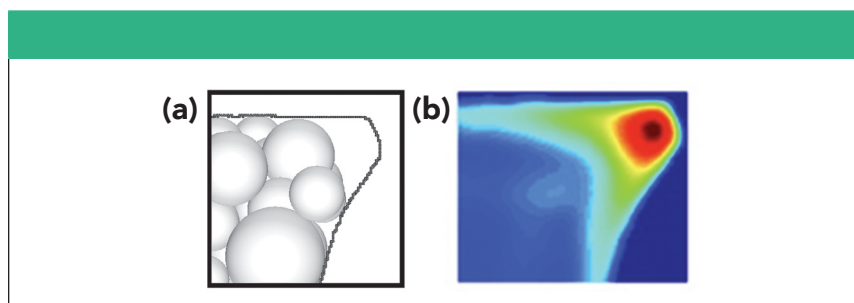


Figure 2: Computational model of (a) random packing in a trapezoidal microfluidic device and (b) fluid dynamic modeling results on the cross-section of the model. The red color in the corner indicates differences in mobile phase velocity in this region compared to the rest of the packed channel. Adapted with permission from (40).

role in maintaining high separation performance. A particle-size segregation effect was also observed in poorer-performing columns. Careful study of the bed morphology showed that smaller particles were more concentrated at the capillary wall and larger particles were more often found closer to the center of the column (Figure 1b). A number of additional studies were then conducted to better understand the cause of this effect, and to determine improved strategies for packing capillary LC columns.

For many years, the approach to packing capillary columns had been to use dilute particle slurry concentrations as a way to reduce particle aggregation and promote a more ordered packed bed (19). However, experiments around the same time of the aforementioned column imaging studies indicated that packing with higher slurry concentrations provided better-performing columns than packing with lower concentrations (20). Comparisons of computationally reconstructed beds based on CLSM images

of columns demonstrated that higher slurry concentrations mitigated the particle size segregation effect during column packing (21). However, very high slurry concentrations resulted in more voids in the packed bed structure that increased band broadening effects. These findings suggested an “optimal” slurry concentration that would simultaneously balance the effects of particle size segregation and void formation, a hypothesis that was later confirmed in studies conducted on a wide range of slurry concentration packing conditions for 75- μm i.d. columns packed with 1.3 μm (22) and 1.9 μm particles (23). Later findings revealed that slurry concentrations above the previously determined optimal level can be used to prepare very efficient columns if sonication is applied to the capillary during the packing process (24). Reduced band broadening and improved column-to-column performance repeatability were observed with this approach, with exceptional reduced plate heights of $h = 1.05$ achieved. These results demonstrate

significant improvements in the preparation of highly efficient packed capillary LC columns, but challenges still remain in the quest for a general set of rules to produce ideal packed column beds. The “optimal” slurry concentration is different for every particle type and column aspect ratio (22), and axial heterogeneity can be a more difficult parameter to fully control (25). Also, many of these findings are specifically applicable to capillary-scale columns; studies to better understand the packing process of analytical-scale LC columns are ongoing (26–30). Finally, because these techniques require specialized, home-built equipment to facilitate the use of packing pressures in excess of 2000 bar, some researchers have instead utilized modified packing protocols with lower pressure requirements (31).

Other Miniaturized Column Formats

The development of packed LC columns in microfabricated devices has been demonstrated in a number of different formats for a variety of applications (32–35). Historically, the challenge with integrating particle-packed beds into microfluidic devices has been that widely used chip fabrication techniques, etching processes from two-dimensional planar designs, create channels with either semi-circular or rectangular cross-sections. In-depth studies on these geometries indicate that shapes containing sharp corners cause a dramatic loss in chromatographic efficiency (36–40). This is primarily due to the difficulty in achieving homogeneous flow profiles across the entire cross section because of the lower packing density that results from not being able to tightly fill these corners with spherical particles (Figure 2). Circular channels can be achieved, but very precise alignment strategies that are challenging to implement are required during device fabrication (41–43), as any minor misalignments can drastically exacerbate broadening. Monolithic columns have been used as an alternative stationary phase in microfluidic channels (44,45), a potential remedy to this issue as the stationary phase can better fill these void areas and reduce porosity differences in corner regions. However, current monolith column technology is most effective for the separation of larger biomolecules and typically exhibits lower plate counts than particle-packed beds for the separation of

RESTEK | ADVANTAGE

See What It Can Do for You and Your Lab

- Technical Articles & Applications
- Videos & ChromaBLOGraphy
- FAQs & Troubleshooting
- Education & Instruction
- Online Tools & Calculators
- Product Selection Assistance

Sign up today to access Restek's years of chromatography knowledge at www.restek.com/advantage



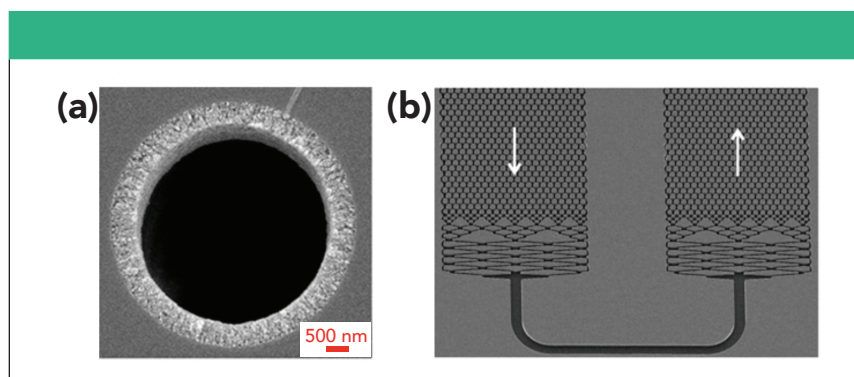


Figure 3: SEM images of (a) an open-tubular capillary LC column with a porous monolith layer at the wall region and (b) a microfabricated pillar array column with flow distributors at the beginning and end of a turn region. Adapted with permission from (57,62).

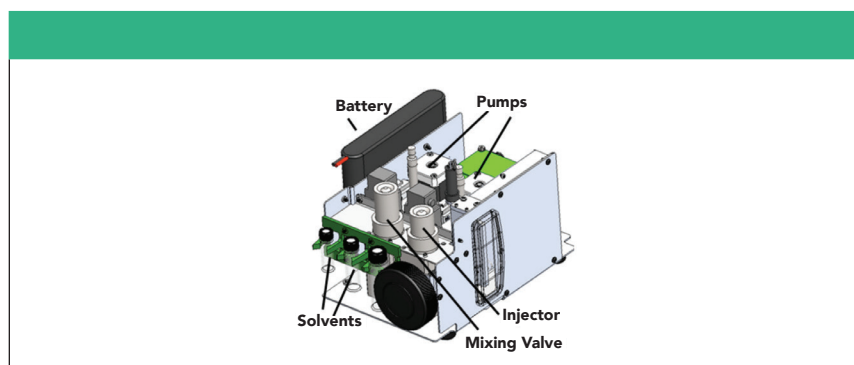


Figure 4: Schematic of the Axcend Focus LC. Adapted with permission from (83).

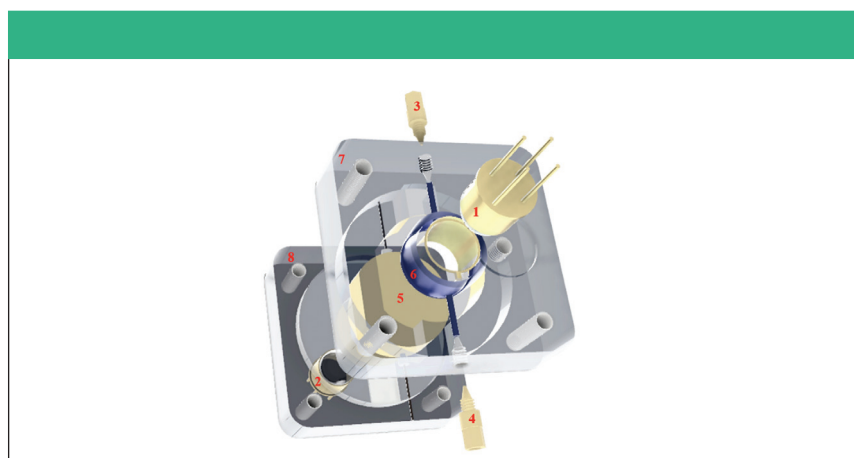


Figure 5: Diagram of a 3D-printed LED-UV detector cell, including 1) UV-LED source, 2) UV photodiode, 3) inlet for coolant flow, 4) outlet for coolant flow, 5) commercial flow cell insert, 6) coolant channel, 7) and 8) cell holders. Adapted with permission from (96).

small molecules (46,47). Both particles and monoliths also suffer from additional issues when adapted to microfluidic platforms. Embedded channel structures often require a “world-to-chip” connection, which must hold pressures above those needed to flow mobile phase through the column at a

reasonable linear velocity. A number of “clamp-like” strategies have shown promise for such a connection (48–52), with a specialized design capable of holding pressures of at least 1700 bar (53). Minimizing total chip footprint is another key to portability, which is often achieved by fabricating

devices with serpentine channels. The addition of sharp turns in packed serpentine channels negatively impacts performance, especially for isocratic separations (53,54). Although the ultimate LC separation device may only be achievable with a completely integrated microfluidic instrument and column (55), many engineering hurdles still remain in the development of such a system.

Other designs for miniaturized capillary-scale columns that provide for more highly-ordered stationary phase support structures can have advantages over packed beds and monoliths. Open-tubular LC (OT-LC) columns provide significant advantages to packed beds by eliminating any efficiency losses due to radial heterogeneity, because there is no packed bed structure (56). Advances in the preparation of these OT-LC columns in recent years have increased the efficiency that can be obtained using the technique (Figure 3a) (57,58), including their use for high-throughput and high-sensitivity separations (59,60). Ordered column structures can also be achieved using microfabricated pillar array columns (61), which can be designed in a variety of geometrical designs to optimize separation efficiency and reduce any potential impacts from wall effects that plague other chromatographic bed structures (Figure 3b) (62–65). The recent commercialization of this pillar array column format has greatly expanded its use for a wide variety of chromatographic applications, especially for the separation of biological molecules (66–69). The current limitation to adapting OT-LC and pillar array columns to portable LC is the decrease in sample loadability due to reduced stationary phase surface area. Although this area can be increased by adding porous monolithic structures onto fused silica walls (70) or etching the surfaces of pillar structures to increase porosity (71), detection modes that are most amenable to lower sample concentrations are still the main choice when using these types of columns. Mass spectrometry (MS) is often utilized, but there are a significant number of challenges when trying to reduce these large MS instruments to hand-portable formats (72). Electrochemical and fluorescence detectors are sensitive detection options that are more amenable to miniaturization (73–75), but they are only responsive to specific analyte classes

unless analyte derivatization is performed (76). The wider utility of absorbance detection for many portable LC applications compared to these other techniques has limited the use of OT-LC and pillar array columns with miniaturized instruments to date, but this is a key opportunity area for future work.

Portable LC Instrument Design

When using capillary LC columns, the biggest challenge often lies with ensuring that the overall instrument system dispersion is low so that it does not significantly impact the separation performance (77–81). Reducing dead volumes in injectors, detector flow cells, and connections between instrument components is critical. Because of the challenges outlined in the preparation of completely microfluidic LC systems, miniaturizing instrument components so that the required fluidic connections and other sources of dispersion in the system are minimized has been a more widely adopted approach in recent years. An added advantage of shrinking down these components is that they can then be combined into integrated, portable LC systems. The key aspects of these systems are that they are small (both in weight and size), contain all necessary electronics and instrument components, can operate on battery or solar power for extended lengths of time, are simple to operate, generate minimal waste, and can achieve performance comparable to benchtop instrumentation (82). As this area of capillary LC instrument development has expanded, four main approaches have been pursued and are detailed here.

The Axcend Focus LC utilizes an integrated capillary column cartridge that can be inserted into a platform containing a pump and injector for tool-free column installation (Figure 4) (83). Flow is generated using two high-pressure syringe pumps that are capable of delivering capillary-scale flow rates up to 690 bar (84,85). The aqueous and organic solvents delivered individually from each pump are combined in a mixing valve. Samples are introduced into a four-port injection valve containing an internal loop in the 4–40 nL range that is compatible with the 150- μm i.d. columns that are incorporated into the cartridge, although the injection valve can be adapted to increase injection volumes up to 700 nL for methods that enhance gradient focusing of the sample at the inlet of the column. Inside the column cartridge, an on-capillary UV absorbance detector utilizing a light-emitting diode (LED) source is fixed directly at the column outlet to eliminate the need for post-column connecting tubing (86,87). A number of applications have been demonstrated using this instrument, including potency and impurity assays for over-the-counter (OTC) pharmaceutical drugs and illicit drug and drug metabolite monitoring (83). Dissolution studies on OTC products have also been performed, with retention time repeatability under 1% RSD across 50 chromatograms collected over 11 h. A prototype version of the platform has also been adapted for coupling to MS systems and used for protein studies (88). More recently, preliminary results for on-line synthetic reaction monitoring (89,90) and beverage quality control (91) were presented. As this system is the first commercially available portable capillary LC instrument, its use is expected to expand in coming years for applications that require remote analysis or the use of small footprint chromatographic instrumentation.

The Australian Centre for Research on Separation Science and the ARC Training Centre for Portable Analytical Separation

Technologies at the University of Tasmania have reported a portable instrument design that uses modular components for LC separations at lower pressures (92–94). Commercially available syringe pumps with pressure limits around 100–120 bar are used for each individual solvent channel, which are combined in a mixing tee and sent to a micro-injection valve (95). A key difference with this instrument is the integration of more standard absorbance flow cells designed for commercial capillary-scale instruments with UV light-emitting diodes (LEDs) in a combined 3D-printed detector interface (Figure 5) (92,96,97). This approach potentially provides enhanced detection limits due to the increased flow cell path length, at the cost of increased detector volume compared to on-capillary detection. To reduce the effect of this larger detector volume on separation performance, the system has been optimized for use with 300- μm i.d. columns. The added benefit of this approach is that slightly higher flow rates can be used with 300- μm i.d. columns, which provided higher retention time reproducibility when using these pumps. Various versions of the system have been applied for the remote analysis of extracted plant materials (92) and environmental monitoring of anions in water using ion chromatography (94).

A third portable capillary LC instrument design, intended to allow for more rugged operation by using gas pressure to generate mobile phase flow, was recently described by the Salehi-Reyhani group (Figure 6) (98). This unique design provided a constant-pressure separation up to 150 bar, driven by a small gas cylinder controlled with a pressure sensor. Because the gas pressure pushes mobile phase from a large reservoir through the column, the length of a single run can be longer than when syringe pumps with a small chamber volume are used, although the use of the reservoir makes



ADVANCING THE SCIENCE OF CHIRAL CHROMATOGRAPHY

DAICEL is committed to advancing chiral chromatography by developing innovative and reliable columns optimized to accelerate your projects.

INTRODUCING CHIRALPAK® IJ

- ✓ DAICEL's newest immobilized chiral stationary phase
- ✓ Robust to withstand all mobile phase combinations
- ✓ Designed for HPLC and SFC to improve methods for challenging separations

WWW.CHIRALTECH.COM



CHIRAL
TECHNOLOGIES INC
DAICEL GROUP

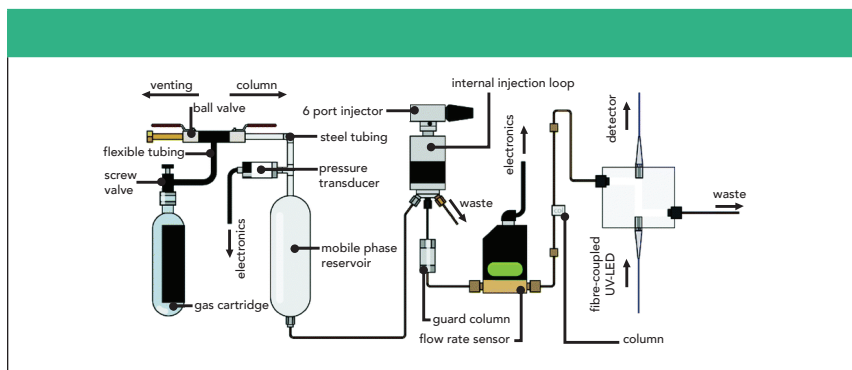


Figure 6: Schematic of a portable LC instrument platform integrating a gas pressure-based pumping mechanism. Adapted with permission from (98).

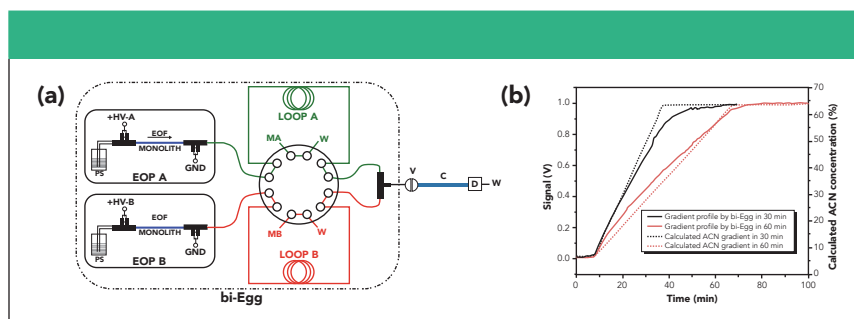


Figure 7: In panel (a), the flow diagram for a binary electroosmotic pump gradient generator (bi-Egg) used for capillary LC is shown. Pumping solution reservoir (PS), input from the high voltage supply (HV), electric ground connection (GND), mobile phase A & B reservoirs (MA, MB), gradient storage loops for each mobile phase component (LOOP A, LOOP B), waste reservoirs (W), injection valve (V), capillary LC column (C), and detector (D) are shown. Panel (b) shows the programmed (dashed line) and observed (solid line) gradient curves for 30 min (black line) and 60 min (red line) linear gradient ramps. Adapted with permission from (104).

the generation of mobile phase gradients much more difficult. As with the two aforementioned portable LC instruments, this system uses an LED-UV absorbance detector. Both particle-packed and monolithic columns were tested with this gas-driven system, but fewer applications have been explored using this instrument, and thus far it has only been applied for the separation of two-component mixtures. The biggest advantage and most impressive result using this system is its robustness under harsh impact conditions. Because of its unique design, the only movable mechanical component is the sample injector, which ensures an added degree of stability compared to more traditional systems. The complete instrument was dropped three times from a height of 1 m while operating, and no significant baseline disturbance was observed any of the times it crashed into the floor. As vibrations might affect various mechanical components during transportation to

remote locations and affect instrument operation for upon arrival, this approach helps minimize this potential issue in portable chromatographic analysis.

Finally, multiple groups have implemented the use of electroosmotic pumping mechanisms for the design of portable LC instruments (99–101). Electroosmotic pumps involve the application of high voltages to charged surface systems (such as fused silica walls, bare silica particles, or silica monoliths) to generate electroosmotic flow (EOF) to pump mobile phase through the column (102). Recent advances have significantly increased the demonstrated pressure limits of these pumps (up to 1200 bar) (103) and their capabilities for generating gradient mobile phase flow (Figure 7) (104,105). An integrated system was demonstrated that combined an electroosmotic pump (including the necessary high-voltage power supplies), an injection valve, and a column (100). It was coupled to an external

UV absorbance detector and a MS detector for the separation of both peptides and proteins, although neither detection mode was portable with this design. A more complete system implemented electroosmotic pumping and used a microfluidic LC column with an LED-based absorbance detector and on-chip valving (101); it was applied for the measurement of glycosylated hemoglobin, a method used for diabetes screening that could be beneficial in resource-limited locations. The use of electroosmotic pumping has significant advantages for the design of miniaturized instruments, especially when utilizing small footprint high-voltage power supplies (106), but challenges for broad applicability remain. The flow rates are highly dependent on the surface chemistry of the EOF pump system, as well as experimental chromatographic parameters including mobile phase selection and column flow resistance. Thus, flexibility for a wide variety of separation conditions and methods is more difficult to achieve than with the syringe-based pumps described for the first two systems.

Conclusions and Future Outlook

The increase of research activity aimed toward the development of higher efficiency capillary-scale chromatographic columns and portable capillary LC instrumentation in recent years demonstrates a push for new separation technology to solve modern problems in chemical analysis. However, without input from prospective users of such technology, it is unlikely that these columns and instruments will find broader acceptance from the greater scientific community. One of the most widely used applications of liquid chromatography is for chemical analysis within the pharmaceutical industry. The Enabling Technologies Consortium (ETC) is a group with membership composed of several major pharmaceutical manufacturers that promotes precompetitive collaborations focused on improved processes for chemical manufacturing and analysis (107). This organization has recently proposed a list of desired instrument capabilities for compact LC technology, demonstrating an interest in pursuing the integration of such instruments into pharmaceutical workflows. Given that the pharmaceutical industry is one of the most critical parts of the greater chromatographic

community, their interest in portable LC instrumentation is a strong indicator of the need for such platforms. This is especially true in the area of process analytical technology (PAT), where real-time feedback based on analytical data acquired directly from the manufacturing process stream is often needed during drug production (108), although continued development in on-line sampling technology is needed to take full advantage of these smaller separation systems (109). Other application areas that will likely benefit from improvements to these portable platforms include forensics (110), point-of-care diagnostics (111), food and beverage testing (112), agricultural analysis (113), and environmental monitoring (114).

Beyond these application areas, there are a variety of instances in which portable instrumentation may be the preferred, or only, way to conduct a LC separation (115). Because of the strict focus on payload weight and volume in space vessels, extra-terrestrial analysis requires the use of miniaturized platforms, especially when conducted remotely to guide additional mission

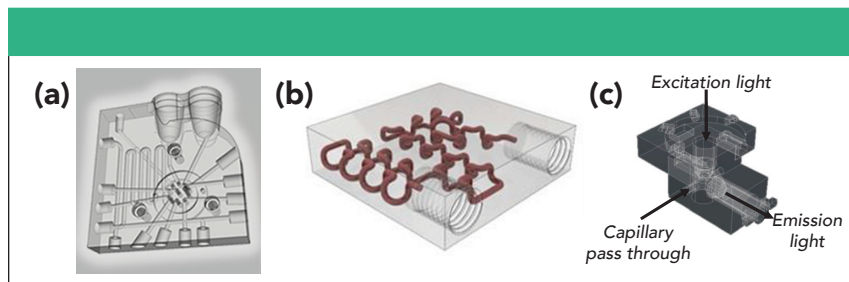
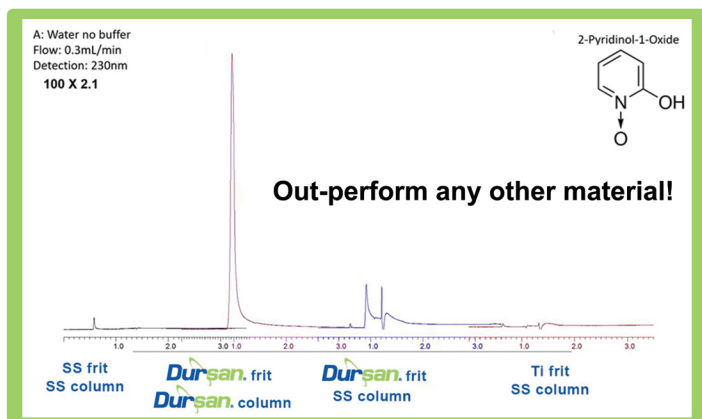


Figure 8: 3D printed designs for (a) manifold enabling in-valve sample handling and assays, (b) 3D serpentine column channel, and (c) an on-column capillary LED-induced fluorescence detector. Adapted with permission from (126,130,136).

tasks (116). This can also be true for difficult-to-reach areas where transportation times are a major hindrance to evaluating samples, such as pollution or commercial testing in isolated ocean sites (117). In air-sensitive environments, such as glove boxes commonly found in laboratories, analysis within the controlled area may be preferred to moving samples in and out of the box for safety and convenience (118); traditional benchtop instrumentation is typically too large to fit in these boxes. Instances where environmental hazards or other issues

related to dangerous exposure may require fast analysis of unknown samples to provide information for defense or public health decision-making are also best served by portable instrumentation (119,120). Direct on-site sampling prevents potential issues in method design and analyte quantification that could result from transporting field samples to the laboratory, which suggests the need for continued progress in on-site sample preparation techniques in parallel to portable instrument design (121). Finally, the added “green” benefit of reduced sol-



Exceed titanium's performance at a fraction of the price.

Reliable, accurate, analytical results.

Save time - no more priming or finding lost peaks.

Make your SS parts bio-inert and eliminate PEEK.

Game-Changing Coatings™
for Better HPLC Analysis



vent use that is achieved through the use of capillary-scale columns (122) is especially pertinent when there is a need to eliminate chemical waste generation in non-laboratory settings.

Both column and instrument design will also be impacted by manufacturing advances enabled by three-dimensional (3D) printing (123–125). Individual instrument components, including valves (126,127), fluidic connections and column platforms (128–133), and detectors (134–136) have all been fabricated using additive manufacturing techniques (Figure 8). The early stages of direct printing of stationary phase supports and column beds have also been reported (137–139), with the ultimate goal of achieving the maximum chromatographic efficiency that is theoretically possible (47,140,141). Although significant challenges to generating an ideal stationary phase support structure for analytical separations in a reasonable time and for a reasonable cost still exist, there are many opportunities for new manufacturing strategies to play a role in the future of chromatographic separations (47,142). Instrument design related to system control and data acquisition may utilize microcontrollers and single-board computers, technology that is often used to control 3D printers, to achieve reduced cost and size in portable instrumentation (143–145).

The potential for smaller chromatographic separation columns and instruments to transform the world of chemical analysis is high. More than fifty years after the initial development of modern HPLC technology, the field has been completely transformed in terms of instrument design, column performance, and analytical throughput. The next step for many chemical measurement techniques involves taking the laboratory to the sample rather than the sample to the laboratory, an approach that can be achieved for LC by implementing many of the advances discussed here. As my research group continues our work in this area, along with the many other separation scientists pursuing the goal of better, faster, and cheaper measurement techniques, we hope to be able to say that the field has completely transformed again 50 years from now!

Acknowledgments

Edward Franklin (Regis Technologies), Justin Godinho (Advanced Materials Technology),

and Kaitlin Grinias (GlaxoSmithKline) are thanked for their helpful discussions regarding these topics. Funding for the Grinias Laboratory on portable LC in collaboration with Axcend Corporation has been supported by the National Institute of Drug Abuse and the National Institute of General Medical Sciences of the National Institutes of Health under award numbers R41DA045382 and R44GM137649. The content is solely the responsibility of the author and does not necessarily represent the official views of the National Institutes of Health.

References

- (1) M.V. Novotny, *J. Chromatogr. A* **1523**, 3–16 (2017).
- (2) J.W. Jorgenson, *Annu. Rev. Anal. Chem.* **3**(1), 129–150 (2010).
- (3) J.E. MacNair, K.C. Lewis, and J.W. Jorgenson, *Anal. Chem.* **69**(6), 983–989 (1997).
- (4) J.E. MacNair, K.D. Patel, and J.W. Jorgenson, *Anal. Chem.* **71**(3), 700–708 (1999).
- (5) L. Tolley, J.W. Jorgenson, and M.A. Moseley, *Anal. Chem.* **73**(13), 2985–2991 (2001).
- (6) K.D. Patel, A.D. Jerkovich, J.C. Link, and J.W. Jorgenson, *Anal. Chem.* **76**(19), 5777–5786 (2004).
- (7) J.S. Mellors and J.W. Jorgenson, *Anal. Chem.* **76**(18), 5441–5450 (2004).
- (8) J.P. Grinias and G.A. Kresge, *LCGC North Am.* **35**(8), 515–516 (2017).
- (9) J.P. Grinias et al., *LCGC North Am.* **38**(2), 75–80 (2020).
- (10) L.E. Blue et al., *J. Chromatogr. A* **1523**, 17–39 (2017).
- (11) A.S. Kaplitz et al., *Anal. Chem.* **92**(1), 67–84 (2020).
- (12) K. Mejía-Carmona, J. Soares da Silva Burato, J.V.B. Borsatto, A.L. de Toffoli, and F.M. Lanças, *TrAC-Trends Anal. Chem.* **122**, 115735 (2020).
- (13) M.J. Sorensen, B.G. Anderson, and R.T. Kennedy, *TrAC-Trends Anal. Chem.* **124**, 115810 (2020).
- (14) S.R. Wilson, C. Olsen, and E. Lundanes, *Anal. Chem.* **144**(24), 7090–7104 (2019).
- (15) S. Bruns et al., *Anal. Chem.* **82**(15), 6569–6575 (2010).
- (16) D. Hlushkou, S. Bruns, A. Höltzel, and U. Tallarek, *Anal. Chem.* **82**(17), 7150–7159 (2010).
- (17) S. Bruns and U. Tallarek, *J. Chromatogr. A* **1218**(14), 1849–1860 (2011).
- (18) S. Bruns, J.P. Grinias, L.E. Blue, J.W. Jorgenson, and U. Tallarek, *Anal. Chem.* **84**(10), 4496–4503 (2012).
- (19) S. Hsieh and J.W. Jorgenson, *Anal. Chem.* **68**(7), 1212–1217 (1996).
- (20) E.G. Franklin, “Utilization of Long Columns Packed with sub-2 μm Particles Operated at High Pressures and Elevated Temperatures for High-Efficiency One-Dimensional Liquid Chromatographic Separations” (2012).
- (21) S. Bruns et al., *J. Chromatogr. A* **1318**, 189–197 (2013).
- (22) A.E. Reising, J.M. Godinho, K. Hormann, J.W. Jorgenson, and U. Tallarek, *J. Chromatogr. A* **1436**, 118–132 (2016).
- (23) A.E. Reising, J.M. Godinho, J.W. Jorgenson, and U. Tallarek, *J. Chromatogr. A* **1504**, 71–82 (2017).
- (24) J.M. Godinho, A.E. Reising, U. Tallarek, and J.W. Jorgenson, *J. Chromatogr. A* **1462**, 165–169 (2016).
- (25) A.E. Reising, J.M. Godinho, J. Bernzen, J.W. Jorgenson, and U. Tallarek, *J. Chromatogr. A* **1569**, 44–52 (2018).
- (26) F. Gritti and M.F. Wahab, *LCGC North Am.* **36**(2), 82–98 (2018).
- (27) M.F. Wahab, D.C. Patel, R.M. Wimalasinghe, and D.W. Armstrong, *Anal. Chem.* **89**(16), 8177–8191 (2017).
- (28) F. Gritti, *J. Chromatogr. A* **1540**, 55–67 (2018).
- (29) A.E. Reising, S. Schlabach, V. Baranau, D. Stoeckel, and U. Tallarek, *J. Chromatogr. A* **1513**, 172–182 (2017).
- (30) F. Gritti, J. Hochstrasser, A. Svidrytski, D. Hlushkou, and U. Tallarek, *J. Chromatogr. A* 460991 (2020). doi:10.1016/j.chroma.2020.460991.
- (31) S.I. Kovalchuk, O.N. Jensen, and A. Rogowska-Wrzęsinska, *Mol. Cell. Proteomics* **18**(2), 383–390 (2019).
- (32) J.P. Kutter, *J. Chromatogr. A* **1221**, 72–82 (2012).
- (33) J.P. Grinias and R.T. Kennedy, *TrAC-Trends Anal. Chem.* **81**, 110–117 (2016).
- (34) A. Kecskemeti and A. Gaspar, *Anal. Chim. Acta* **1021**, 1–19 (2018).
- (35) X. Yuan and R.D. Oleschuk, *Anal. Chem.* **90**(1), 283–301 (2018).
- (36) S. Khirevich, A. Höltzel, D. Hlushkou, and U. Tallarek, *Anal. Chem.* **79**(24), 9340–9349 (2007).
- (37) S. Ehlert et al., *Anal. Chem.* **80**(15), 5945–5950 (2008).
- (38) S. Khirevich, A. Höltzel, D. Hlushkou, A. Seidel-Morgenstern, and U. Tallarek, *Lab Chip* **8**(11), 1801–1808 (2008).
- (39) S. Jung et al., *Anal. Chem.* **81**(24), 10193–10200 (2009).
- (40) S. Khirevich, A. Höltzel, S. Ehlert, A. Seidel-Morgenstern, and U. Tallarek, *Anal. Chem.* **81**(12), 4937–4945 (2009).

- (41) W. Wang et al., *Anal. Chem.* **86**(4), 1958–1964 (2014).
- (42) S. Wang et al., *Anal. Chim. Acta* **1018**, 70–77 (2018).
- (43) K. Li et al., *Talanta* **215** (2020).
- (44) M. Vázquez and B. Paull, *Anal. Chim. Acta* **668**(2), 100–113 (2010).
- (45) R. Knob, V. Sahore, M. Sonker, and A.T. Woolley, *Biomicrofluidics* **10**(3) (2016).
- (46) D. Cabooter et al., *J. Chromatogr. A* **1325**, 72–82 (2014).
- (47) K. Broeckhoven et al., *LCGC North Am.* **36**(6), 9–17 (2018).
- (48) A.G. Chambers, J.S. Mellors, W.H. Henley, and J.M. Ramsey, *Anal. Chem.* **83**(3), 842–849 (2011).
- (49) S. Wouters et al., *J. Chromatogr. A* **1355**, 253–260 (2014).
- (50) S. Wouters et al., *J. Chromatogr. A* **1523**, 224–233 (2017).
- (51) J.P. Grinias and R.T. Kennedy, *Chromatography* **2**(3), 502–514 (2015).
- (52) C. Lotter et al., *Anal. Chem.* **88**(15), 7481–7486 (2016).
- (53) M. Gilar et al., *J. Chromatogr. A* **1533**, 127–135 (2018).
- (54) M. Gilar, T.S. McDonald, and F. Gritti, *J. Chromatogr. A* **1470**, 76–83 (2016).
- (55) F. Gritti and G. Guiochon, *J. Chromatogr. A* **1228**, 2–19 (2012).
- (56) S.C. Lam, E. Sanz Rodriguez, P.R. Haddad, and B. Paull, *Analyst* **144**(11), 3464–3482 (2019).
- (57) T. Hara et al., *Anal. Chem.* **88**(20), 10158–10166 (2016).
- (58) T. Hara et al., *J. Chromatogr. A* **1580**, 63–71 (2018).
- (59) P. Xiang, Y. Yang, Z. Zhao, M. Chen, and S. Liu, *Anal. Chem.* **91**(16), 10738–10743 (2019).
- (60) P. Xiang et al., *Anal. Chem.* **92**(7), 4711–4715 (2020).
- (61) G. Desmet and S. Eeltink, *Anal. Chem.* **85**(2), 543–556 (2013).
- (62) W. De Malsche, J. Op De Beeck, S. De Bruyne, H. Gardeniers, and G. Desmet, *Anal. Chem.* **84**(3), 1214–1219 (2012).
- (63) G. Desmet, M. Callewaert, H. Ottevaere, and W. De Malsche, *Anal. Chem.* **87**(14), 7382–7388 (2015).
- (64) S. Futagami et al., *Analyst* **144**(5), 1809–1817 (2019).
- (65) M. Baca, G. Desmet, H. Ottevaere, and W. De Malsche, *Anal. Chem.* **91**(17), 10932–10936 (2019).
- (66) K. Sandra et al., *LCGC North Am.* **30**(6s), 6–13 (2017).
- (67) G. Nys, G. Cobraiville, and M. Fillet, *Anal. Chim. Acta* **1086**, 1–13 (2019).
- (68) J. Stadlmann et al., *Anal. Chem.* **91**(22), 14203–14207 (2019).
- (69) G. Tóth, T. Panić-Janković, and G. Mitulović, *J. Chromatogr. A* **1603**, 426–432 (2019).
- (70) T. Hara, S. Futagami, W. De Malsche, G.V. Baron, and G. Desmet, *J. Chromatogr. A* **1552**, 87–91 (2018).
- (71) S. Futagami et al., *J. Chromatogr. A* **1595**, 58–65 (2019).
- (72) D.T. Snyder, C.J. Pulliam, Z. Ouyang, and R.G. Cooks, *Anal. Chem.* **88**(1), 2–29 (2016).
- (73) X. Xu, L. Li, and S.G. Weber, *TrAC-Trends Anal. Chem.* **26**(1), 68–79 (2007).
- (74) M. Macka, T. Piasecki, and P.K. Dasgupta, *Annu. Rev. Anal. Chem.* **7**(1), 183–207 (2014).
- (75) M. Zhang, S.C. Phung, P. Smejkal, R.M. Guijt, and M.C. Breadmore, *Trends Environ. Anal. Chem.* **18**, 1–10 (2018).
- (76) C.F. Poole, in *Liquid Chromatography Applications*, S. Fanali, P.R. Haddad, C.F. Poole, and

HPLC Columns for Organic Acid Analysis

Over 40 years of experience providing high quality polymeric HPLC columns for the analysis of samples containing carbohydrates and organic acids.



 **Benson**
polymeric™



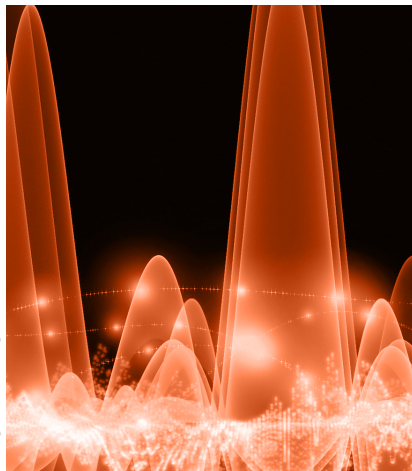
bensonpolymeric.com
775.356.5755

- M-L. Riekkola, Eds. (Elsevier, Amsterdam, Netherlands, 2nd Ed., 2017), pp. 39–68.
- (77) E. Vasconcelos Soares Maciel, A.L. de Toffoli, E. Sobieski, C.E. Domingues Nazário, and F.M. Lanças, *Anal. Chim. Acta* **1103**, 11–31 (2020).
- (78) K.B. Lynch, A. Chen, and S. Liu, *Talanta* **177**, 94–103 (2018).
- (79) G. Desmet and K. Broeckhoven, *TrAC Trends Anal. Chem.* **119**, 115619 (2019).
- (80) J.P. Grinias, B. Bunner, M. Gilar, and J.W. Jorgenson, *Chromatography* **2**(4), 669–690 (2015).
- (81) E.G. Franklin and T.W. Kahler, *LCGC North Am.* **34**(6), 388–399 (2016).
- (82) S. Sharma et al., *J. Chromatogr. A* **1421**, 38–47 (2015).
- (83) S.W. Foster et al., *J. Sep. Sci.* **43**, 1623–1627 (2020).
- (84) S. Sharma et al., *J. Chromatogr. A* **1327**, 80–89 (2014).
- (85) S. Sharma et al., *Anal. Chem.* **87**(20), 10457–10461 (2015).
- (86) S. Sharma, H.D. Tolley, P.B. Farnsworth, and M.L. Lee, *Anal. Chem.* **87**(2), 1381–1386 (2015).
- (87) X. Xie et al., *J. Chromatogr. A* **1523**, 242–247 (2017).
- (88) X. Zhao et al., *Anal. Chem.* **89**(1), 807–812 (2017).
- (89) X. Xie, L. Patil, and M. Lee, “Utilizing Portable Capillary LC for Automated On-line Process and Reaction Monitoring” at Pittcon 2020 (Chicago, IL, 2020).
- (90) M. Lee et al., “Breadth of Applications of Portable Capillary Liquid Chromatography” at Pittcon 2020 (Chicago, IL, 2020).
- (91) J.P. Grinias, S. Foster, M. Pham, and G. Kresge, “The Potential for Portable Liquid Chromatography in Chemical Analysis” at Pittcon 2020 (Chicago, IL, 2020).
- (92) S.C. Lam et al., *Anal. Chim. Acta* **1101**, 199–210 (2020).
- (93) Y. Li et al., *Anal. Chim. Acta* **896**, 166–176 (2015).
- (94) E. Murray et al., *J. Sep. Sci.* **41**(16), 3224–3231 (2018).
- (95) Y. Li et al., *Talanta* **180**, 32–35 (2018).
- (96) S. C. Lam, V. Gupta, P. R. Haddad, and B. Paull, *Anal. Chem.* **91**(14), 8795–8800 (2019).
- (97) Y. Li, P.N. Nesterenko, R. Stanley, B. Paull, and M. Macka, *Anal. Chim. Acta* **1032**, 197–202 (2018).
- (98) S. Chatzimichail, D. Casey, and A. Salehi-Reyhani, *Analyst* **144**(21), 6207–6213 (2019).
- (99) A. Ishida et al., *Anal. Sci.* **31**(11), 1163–1169 (2015).
- (100) K.B. Lynch, A. Chen, Y. Yang, J.J. Lu, and S. Liu, *J. Sep. Sci.* **40**(13), 2752–2758 (2017).
- (101) D. Li et al., *Sensors Actuators, B Chem.* **305**, 127484 (2020).
- (102) L. Li, X. Wang, Q. Pu, and S. Liu, *Anal. Chim. Acta* **1060**, 1–16 (2019).
- (103) C. Gu et al., *Anal. Chem.* **84**(21), 9609–9614 (2012).
- (104) I.L. Zhou, J.J. Lu, C. Gu, and S. Liu, *Anal. Chem.* **86**(24), 12214–12219 (2014).
- (105) A. Chen et al., *Anal. Chim. Acta* **887**, 230–236 (2015).
- (106) P. Kubáň, F. Foret, and G. Erny, *Electrophoresis* **40**(1), 65–78 (2019).
- (107) C.J. Welch et al., *Org. Process Res. Dev.* **21**(3), 414–419 (2017).
- (108) A. Chanda et al., *Org. Process Res. Dev.* **19**(1), 63–83 (2015).
- (109) C.A. Challener, *Pharm. Technol.* **41**(4), 22–27 (2017).
- (110) W.R. de Araujo et al., *Anal. Chim. Acta* **1034**, 1–21 (2018).
- (111) M. Zarei, *TrAC-Trends Anal. Chem.* **91**, 26–41 (2017).
- (112) G. Rateni, P. Dario, and F. Cavallo, *Sensors* **17**(6), 1453 (2017).
- (113) A. Casedy, E. Mullins, and R. O’Kennedy, *Biotechnol. Adv.* **39** (2020).
- (114) R. Pol, F. Céspedes, D. Gabriel, and M. Baeza, *TrAC-Trends Anal. Chem.* **95**, 62–68 (2017).
- (115) M. Kaljurand, *Trends Environ. Anal. Chem.* **1** (2014).
- (116) C.P. Shelor et al., *Astrobiology* **14**(7), 577–588 (2014).
- (117) J. Birch, *Pure Appl. Chem.* **90**(10), 1625–1630 (2018).
- (118) D.J. Leggett, *Process Saf. Prog.* **31**(4), 393–397 (2012).
- (119) I.S. Che Sulaiman et al., *Forensic Toxicol. Dec.* **16** (2019). doi:10.1007/s11419-019-00513-x.
- (120) R. Jackson and B.A. Logue, *Anal. Chim. Acta* **960**, 18–39 (2017).
- (121) J. Pawliszyn, *TrAC-Trends Anal. Chem.* **25**(7), 633–634 (2006).
- (122) J. Plotka et al., *J. Chromatogr. A* **1307**, 1–20 (2013).
- (123) U. Kalsoom, P. N. Nesterenko, and B. Paull, *TrAC-Trends Anal. Chem.* **105**, 492–502 (2018).
- (124) B. Paull, *LCGC Europe* **30**(11), 611–612 (2017).
- (125) S. Dimartino, *LCGC Europe* **32**(6), 317–318 (2019).
- (126) D.J. Cocovi-Solberg, M. Rosende, M. Michalec, and M. Miró, *Anal. Chem.* **91**(1), 1140–1149 (2019).
- (127) S.H. Nawada, T. Aalbers, and P.J. Schoenmakers, *Chem. Eng. Sci.* **207**, 1040–1048 (2019).
- (128) S. Sandron et al., *Analyst* **139**(24), 6343–6347 (2014).
- (129) V. Gupta et al., *Anal. Chim. Acta* **910**, 84–94 (2016).
- (130) V. Gupta, S. Beirne, P. N. Nesterenko, and B. Paull, *Anal. Chem.* **90**(2), 1186–1194 (2018).
- (131) T. Adamopoulou, S. Deridder, G. Desmet, and P.J. Schoenmakers, *J. Chromatogr. A* **1577**, 120–123 (2018).
- (132) M. Komendová, S. Nawada, R. Metelka, P.J. Schoenmakers, and J. Urban, *J. Chromatogr. A* **1610** (2020).
- (133) M. Passamonti et al., *Anal. Chem.* **92**(3), 2589–2596 (2020).
- (134) J. Prikryl and F. Foret, *Anal. Chem.* **86**(24), 11951–11956 (2014).
- (135) F. Cecil et al., *Anal. Chim. Acta* **965**, 131–136 (2017).
- (136) L.D. Casto, K.B. Do, and C.A. Baker, *Anal. Chem.* **91**(15), 9451–9457 (2019).
- (137) R.J. Vonk, A. Vaast, S. Eeltink, and P.J. Schoenmakers, *J. Chromatogr. A* **1359**, 162–169 (2014).
- (138) C. Fee, S. Nawada, and S. Dimartino, *J. Chromatogr. A* **1333**, 18–24 (2014).
- (139) S. Nawada, S. Dimartino, and C. Fee, *Chem. Eng. Sci.* **164**, 90–98 (2017).
- (140) C. Salmean and S. Dimartino, *Chromatographia* **82**(1), 443–463 (2019).
- (141) F. Dolamore, S. Dimartino, and C. J. Fee, *Anal. Chem.* **91**(23), 15009–15016 (2019).
- (142) G. Desmet, “Hot Topics in HPLC Part II: The Possibilities and Challenges of Producing Chromatographic Media with Two-Photon Polymerization Printing LC–GC” (2020). at <http://www.chromatographyonline.com/hot-topics-hplc-part-ii>.
- (143) J.P. Grinias, J.T. Whitfield, E.D. Guetschow, and R.T. Kennedy, *J. Chem. Educ.* **93**(7), 1316–1319 (2016).
- (144) S.W. Foster, M.J. Alirangues, J.A. Naese, E. Constans, and J.P. Grinias, *J. Chromatogr. A* **1603**, 396–400 (2019).
- (145) P.L. Urban, *Angew. Chemie - Int. Ed.* **57**(34), 11074–11077 (2018).

James P. Grinias is an assistant professor in the Department of Chemistry & Biochemistry at Rowan University, in Glassboro, New Jersey. Direct correspondence to: grinias@rowan.edu

Biocompatible Microextraction Devices for Simple and Green Analysis of Complex Systems

Image credit: agandrew/stock.adobe.com



For many decades, fast and reliable analysis of complex matrices, such as food, biofluids, or environmental samples, has been a challenge to the analytical chemistry community. In spite of the significant progress achieved so far in terms of analytical instrumentation and data deconvolution software, the pretreatment of complex samples still represents a key step in the analytical workflow that critically impacts the overall quality of results acquired. Microextraction, with its multifaceted modes and configurations, has played an essential role in enabling simpler pretreatment of challenging complex matrices to facilitate instrumental analysis. In this article, the development and evolution of biocompatible solid-phase microextraction (bio-SPME) are discussed, with special emphasis on extraction phases suitable for liquid chromatography and direct mass spectrometry applications. Some of the unique applications enabled by bio-SPME devices over the years are also described.

As a sample preparation technique, solid-phase microextraction (SPME) has evolved tremendously since its inception in 1990 (1,2). Initially designed for thermal desorption and gas-chromatography (GC) applications, SPME revolutionized the philosophy of sample preparation and extraction, as it enabled the simultaneous extraction and preconcentration of analytes from a given matrix (3). In the 1990s, especially after the commercialization of SPME devices by Supelco (now MilliporeSigma, the Life Science business of Merck KGaA, Darmstadt, Germany), their use as sample preparation tools in the field of aroma and fragrances determination, and the extraction of GC-amenable organics from noncomplex water samples increased significantly (4). Thermal desorption of SPME devices was the optimal solution for GC applications, because it was compatible with the GC-injector port without extensive modification of the existing hardware (apart from the inner glass liner that required narrower internal diameter for SPME applications) (5).

In terms of extraction phase chemistry, a common polymer used as a stationary phase into GC columns was selected for its good sorption properties and its thermal stability: polydimethylsiloxane (PDMS). Consequently, PDMS-based SPME coatings were first commercialized, and are still to date the most commonly used extraction phases for SPME. To expand the use of the technique for the analysis of nonvolatile analytes via liquid chromatography (LC), desorption strategies using solvent systems with high affinity for the analytes of interest were implemented. The desorption solvent containing the analytes can then be injected into the LC system directly or after preconcentration or reconstitution, if necessary. Considering that molecular mass transfer in the liquid phase is slower in comparison to the gas phase, quantitative solvent desorption generally takes longer than thermal desorption. Because solvent desorption is typically performed off-line, agitation can be used to speed up the process. Two important factors to take into consideration when performing SPME via LC are that the

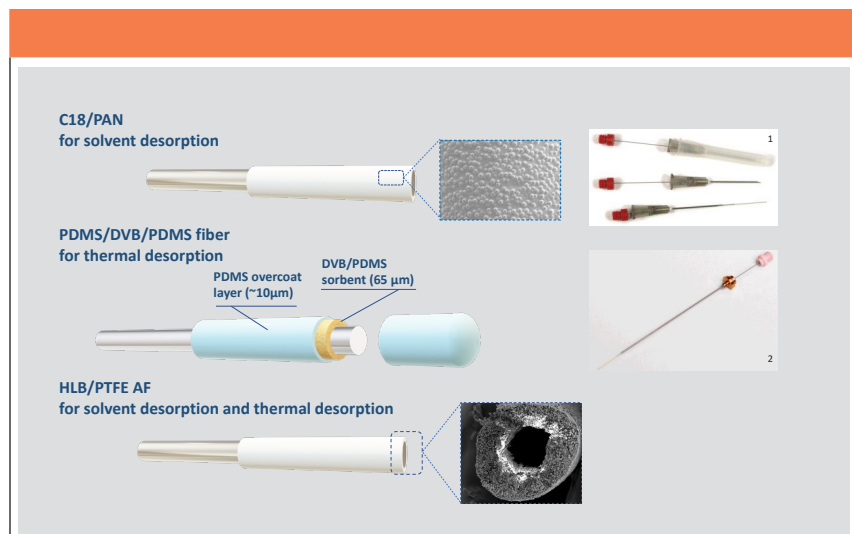


Figure 1: Schematic representation of biocompatible SPME fibers. Images 1 and 2 are partially reproduced from sigmaaldrich.com. Objects not to scale for optimal visual representation.

desorption solution should enable quantitative desorption of the analytes (and consequently avoid carryover), and the final extract should be compatible with the mobile phase composition. Often, to meet these two requirements and also to preconcentrate the extracts, the desorption solvent system can be evaporated and reconstituted with an appropriate solvent system.

In terms of extraction modes, SPME for GC applications could be performed in either headspace (HS) or direct immersion (DI), based on the volatility of the target analytes. For complex matrices, HS-SPME was usually preferred to avoid exposing the SPME device directly to the sample. Performing DI-SPME in complex matrices can likely lead to the attachment of matrix constituents to the extraction phase surface, affecting the extraction efficiency of the device and subsequently reducing its lifetime. When DI-SPME was necessary, many researchers opted for pretreating the matrix with methods including, but not limited to, dilution, centrifugation, and filtration. Although these sample pretreatment strategies were effective, most often they defeated the scope of the simple and one-step extraction process that SPME is able to provide.

Expanding the applicability of SPME to LC-based approaches posed a challenge to the technology: LC-amenable analytes are semi- or non-volatile, therefore direct immersion SPME (DI-SPME) is manda-

tory. Given that extensive sample pretreatment is not practical, and can potentially induce analyte loss and lack of reproducibility, alternative extraction devices were urgently needed.

In light of these factors, significant research efforts were devoted to the development of “biocompatible” or “matrix compatible” SPME extraction phases, with both descriptions referring to the SPME coating’s anti-fouling characteristics (6–8). It is also worth mentioning that biocompatible SPME devices are manufactured with materials that are non-toxic and non-injurious to a living system, thus enabling the applicability of the technique also for in-vivo sampling (9–12).

The manufacture of biocompatible SPME devices must take into account various aspects for optimal extraction performance.

First, the outer surface of the SPME extraction phase represents the boundary phase that lies between the bulk of the matrix and the inner sorbent material. Interactions between the material and the sample matrix occur chiefly on such surface. The performance of a polymeric material for biocompatible SPME devices must have a good ability to prevent attachment of macromolecules (such as proteins and other biomolecules), and should permit smaller molecules to permeate its surface to reach the sorbent material in a reasonable time.

Second, pure polymers with antifouling properties do not always guarantee adequate extraction efficiency. Therefore, sorp-

tive materials need to be incorporated to enhance the extraction performance. Most of these sorbents, however, are not biocompatible, so their surface must be surrounded by the antifouling polymer at the interface with the sample matrix.

Consequently, the first biocompatible extraction phase used for SPME-LC applications consisted of polyacrylonitrile (PAN), an antifouling polymer that also works as a binder to immobilize sorbents such as C18 functionalized silica particles (6). PAN and acrylonitrile-based copolymers are hydrophilic polymers broadly used in the biomedical field as membrane materials for dialysis, ultrafiltration, enzyme-immobilization, and pervaporation, due to their anti-biofouling properties and chemical stability.

The applicability of biocompatible SPME devices for biofluids and tissue analysis is highly dependent on the ability of the biocompatible polymer to prevent attachment of proteins that can affect the mass transfer of smaller organic molecules into the sorbent and act as anchors for the attachment of cells (for example, blood cells) (6). PAN, like other hydrophilic polymers, prevents the adhesion of fouling agents through the formation of a physical barrier known as hydration layer (13,14). The hydration layer is formed by hydrogen bonding between the functional groups on the device surface and water molecules in the sample matrix. The applicability of PAN for LC-based SPME devices also relies on its good binding ability toward sorptive particles to create a homogeneous slurry that can be applied as very thin layers. This feature facilitates the fabrication of devices that can be applied for in vivo and tissue analysis with improved mass transfer across the thin coating layers. Moreover, the good chemical stability of PAN toward most organic solvent facilitates solvent desorption without damaging or swelling the extraction phase, even if long desorption times are required. These unique properties make PAN-based extraction devices a very convenient solution for complex biofluids and tissue analysis that minimizes the effect of matrix interferences. PAN-based SPME devices are currently commercially available from MilliporeSigma, the Life Science business of Merck KGaA, Darmstadt, Germany (Figure 1).

Typical steps in the workflow of SPME-LC analysis of complex biospecimens by PAN-based SPME devices are as follows:

- 1) **Preconditioning.** This step is generally needed to activate the sorbent particles prior to extraction, and it is performed with a solution of water and organic solvent (commonly 1:1 (v:v) MeOH:H₂O for 15-30 min).
- 2) **Rinsing.** Prior to extraction in complex biomatrices, it is critical to quickly rinse the SPME device in pure water (30 s). This helps to remove residual organic solvent after the preconditioning step, which may induce protein precipitation on the device surface during extraction.
- 3) **Extraction.** PAN-based biocompatible coatings can be directly exposed to untreated biofluids and tissues. Depending on the objective, the extraction time may be tuned toward maximum extraction recovery where sensitivity is pertinent or minimized for faster throughput.
- 4) **Post-extraction rinsing.** Prior to desorption, it is a useful practice to quickly rinse the SPME device to remove any matrix component that can potentially be left loosely attached on its surface; this will further prevent matrix contamination. However, care must be taken not to compromise the overall amount of extracted analytes.
- 5) **Solvent desorption.** During solvent desorption, the analytes need to be desorbed in a solvent system strong enough to reverse the interaction of analytes with the extraction phase. In SPME-LC, the desorption solvent ideally should match the initial composition of the mobile phase to avoid solvent mismatch and poor chromatography. When this is not achievable, evaporation of the desorption solution and reconstitution with proper solvent combinations are recommended.
- 6) **Cleanup (optional, if the devices are being re-used).** Cleanup can be performed to prepare the SPME for the next cycle of extraction in the case of extraction from very complex matrices or to make sure all the analytes extracted are fully desorbed.

PAN-based SPME extraction phases have enabled a cascade of applications including in-vivo metabolomics in the brain, liver, lungs, and in various biofluids (15–22). Moreover, the easy applicability of PAN-based extraction phases onto supports of different geometries permitted the development of multiple microextraction tools,

compatible with various sampling needs (such as recessed SPME [23,24], single-use samplers coated on plastic supports [25,26]) and to direct coupling to mass spectrometry (transmission mode SPME [27–29], nano-spray [30], and coated blade spray [31–35], being commercialized by Restek Corporation).

Although PAN-based extraction phases are well suited for solvent desorption, the lack of thermal stability above 120–160 °C does not make them suitable for SPME-GC applications due to the high temperatures needed for effective thermal desorption (36).

In light of this, and to expand the appli-

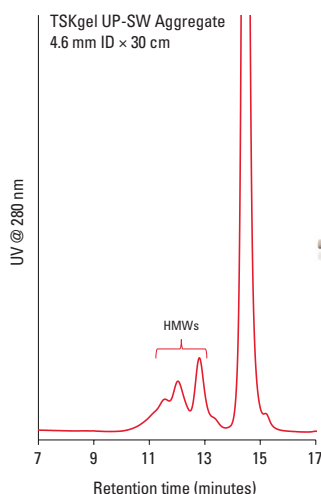
cability of DI-SPME-GC in complex matrices, a novel biocompatible (or matrix compatible) extraction phase was developed (8). This extraction phase was optimized based on commercially available SPME fibers for GC applications; it was noticed that pure PDMS extraction phases endured direct immersion into complex and untreated food matrices for longer series of extractions without noticeable coating fouling while maintaining good extraction efficiency. PDMS is well known for being a hydrophobic biocompatible polymer that prevents the formation of hydrogen bonds, thus avoiding

Introducing...

TSKgel® UP-SW Aggregate 3 μm, 30 nm Size Exclusion Chromatography Columns

**Ideal for the separation of mAb aggregates,
high molecular weight proteins and nucleic acids.**

- 30 nm pore size with separation range of 10-2,000 kDa
- Compatible with both HPLC and UHPLC systems
- Provides high sensitivity and excellent column efficiency
- Proven TSKgel SW SEC quality – latest addition to UP-SW series of columns



The TSKgel UP-SW Aggregate column allows a more detailed view on the high order aggregates.



Tosoh Bioscience and TSKgel are registered trademarks of Tosoh Corporation.

TOSOH BIOSCIENCE
www.tosohbioscience.com



the attachment of water and biomolecules alike (13). However, PDMS extraction efficiency is limited by its hydrophobicity. Thus, to obtain extraction phases able to provide a broader extraction range, commercial SPME devices were manufactured using PDMS as a binder for sorbents such as divinyl benzene (DVB), Carboxen (Car), and a mixture of these (4). The incorporation of sorbent particles, however, affected the outer morphology of the extraction phase compared to pure PDMS devices, making them uneven and rough. This issue was found to be detrimental when SPME devices were used for the analysis of complex matrices via DI, as residues of matrix constituents accumulate on the interstices of the extraction phase surface, and then get carbonized during thermal desorption. Subsequently, this leads to fouling buildup that would reduce the device's extraction efficiency and affect its reusability. To overcome this issue, the design of the new PDMS/DVB/PDMS extraction phase included a thin and smooth layer of pure PDMS (~10 μm) to protect conventional commercial SPME devices such as a DVB/PDMS fibers (8). The new design, presented in Figure 1, enabled direct immersion in very complex matrices such as foodstuffs, without the need for extensive sample pretreatment. This extraction phase demonstrated its efficacy especially for fruit and vegetable analysis; the significant presence of carbohydrates in these matrices affected conventional SPME device performance. In fact, carbohydrate residues on the surface of the coating carbonize during thermal desorption, damaging the extraction phase irreversibly, and creating artifacts that will populate the chromatogram, potentially masking targeted analytes. The development of this new extraction phase enabled several applications in diverse food matrices for both targeted and untargeted analysis, including *in vivo* applications in fruits (37–41). In addition, the ability to add rinsing and washing steps in the analytical workflow was generally found to prolong the coating lifetime. For example, in the case of matrices with high water and carbohydrates content, a post-extraction rinsing in pure water (5–20 sec) was found effective to guarantee coating cleanness and to avoid the occurrence of artifacts due to thermal conversion of sugars into the GC injector (41). For the same matrix types, post-desorption washing in water:methanol 1:1 (v:v) also showed efficacy in removing

any matrix residue on the extraction phase surface. For food matrices with high-fat content, different rinsing and washing strategies must be developed to remove oily residues from the SPME device surface to prevent extensive contamination of the GC injector. Complex matrices, such as avocado, soy milk, and dried seaweed, require a mixture of acetone and water, at different ratios, to be used for both rinsing and washing solutions (37,39,40). It is important to mention that special attention should be paid when performing the rinsing step, especially if solvents other than water are used. The rinsing time in these cases must be kept as short as possible, to minimize analyte losses. However, this phenomenon does not apply to washing procedures performed after desorption process. It is also critical to select solvents that do not affect the structural integrity of the fiber; chlorinated solvents and hydrocarbon-based solvents are known to swell PDMS.

Since their inception, PAN- and PDMS-based biocompatible coatings have facilitated the analysis of complex matrices by SPME, providing unique analytical solutions for both targeted and untargeted analysis of food, environmental, and biosamples. However, these extraction phases are specific to different separation platforms: LC in the case of PAN-based devices and GC for PDMS-devices. Therefore, sampling of complex matrices for extraction of both LC- and GC-amenable analytes could be further improved by a biocompatible SPME extraction phase compatible with both thermal and solvent desorption mechanisms.

Fluorinated polymers constitute a unique class of materials with high chemical resistance and thermal stability. This class of polymers is known to be chemically inert or relatively unreactive. Polytetrafluoroethylene (PTFE), also known by its trade name Teflon, is the first fluoropolymer to be discovered in 1938 and exhibits exceptional ability to repel water, oils, adhesives, and so on (42). Moreover, it is a well-established biocompatible material, often used for the production of medical devices. One major disadvantage in the use of PTFE is that it is not soluble and does not swell in most solvents, thus machining techniques are commonly used to process it. To overcome this limitation, amorphous fluoropolymers such as PTFE-AF were developed. PTFE-AF is a copolymer of tetrafluoroethylene and 2,2-bis(trifluoromethyl)-4,5-difluoro-1,3-di-

oxole, and exhibits improved mechanical stability and high solubility in fluorinated solvents. Moreover, the fluorinated backbone of PTFE-AF provides similar biocompatibility and stability as the PTFE polymer (42). These characteristics make PTFE-AF an excellent candidate for the manufacturing of biocompatible SPME devices suitable for both solvent and thermal desorption. The first report of receptor-doped fluorinated films for SPME was reported in 2014 (43), followed by the fabrication of PTFE-AF-based SPME fiber that incorporated hydrophilic-lipophilic balance particles (HLB) in 2017 (44). This HLB-PTFE-AF extraction phase was specifically designed to serve as a multipurpose sampling tool for complex matrices. Although the PTFE-AF guaranteed compatibility to LC and GC desorption techniques, the HLB particles provided broader extraction coverage, and improved recovery for more polar analytes. The compatibility with different chromatographic platforms together with the collection of a broader range of analytes make this extraction phase well suited for untargeted analysis. This new biocompatible extraction phase was tested for the extraction of a broad range of LC and GC amenable analytes in biofluids such as whole blood, saliva, serum, and urine, and in Concord grape juice, a food matrix particularly challenging for its high content in sugars and pigments. When repetitive DI-SPME extraction/desorption cycles were performed prior to GC and LC analysis from the matrices mentioned above, good performance was achieved up to at least 50 consecutive cycles for both solvent and thermal desorption techniques. Moreover, it was assessed that the chemistry of this new extraction phase and in particular the inertness of the PTFE-AF material, drastically minimizes the impact of the matrix on the overall analytical process (45).

Conclusion

In summary, the introduction of biocompatible extraction phases has significantly expanded the applicability of the SPME technology and enabled convenient analysis of complex matrices with minimum or no sample pretreatment. This results in numerous advantages in terms of the throughput of the analytical routine and minimization of laboratory waste production. Additionally, the unique properties of these SPME devices together with their miniaturized geometry

offer exceptional sampling opportunities applicable to in-vivo analysis.

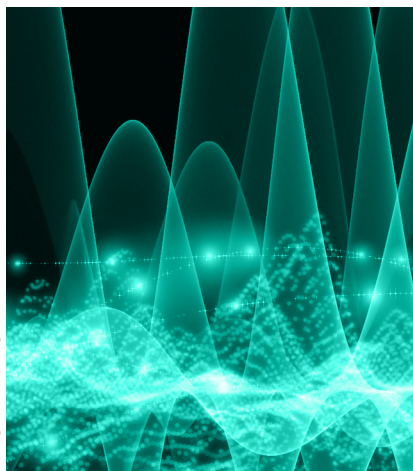
References

- (1) C.L. Arthur and J. Pawliszyn, *Anal. Chem.* **62**(19), 2145–2148 (1990). doi:10.1021/ac00218a019
- (2) N. Reyes-Garcés, E. Gionfriddo, G.A. Gómez-Ríos, M.N. Alam, E. Boyaci, B. Bojko, V. Singh, J. Grandy, and J. Pawliszyn, *Anal. Chem.* **90**(1), 302–360 (2018). doi:10.1021/acs.analchem.7b04502
- (3) J. Pawliszyn, *Handbook of Solid Phase Microextraction* (Elsevier, Waltham, Massachusetts, 2012).
- (4) J. Pawliszyn, *Development of SPME Devices and Coatings in Handbook of Solid Phase Microextraction* (Elsevier, Waltham, Massachusetts, 2012), pp. 61–97
- (5) J. Pawliszyn, L. Kudlejova, S. Risticicvic, and D. Vuckovic, *Handbook of Solid Phase Microextraction* (Elsevier, Waltham, Massachusetts, 2012), pp. 201–249
- (6) M. L. Musteata, F. M. Musteata, and J. Pawliszyn, *Anal. Chem.* **79**(18), 6903–6911 (2007). doi:10.1021/ac70296s
- (7) N. H. Godage and E. Gionfriddo, *TrAC Trends Anal. Chem.* **111**, 220–228 (2019). doi:10.1016/j.trac.2018.12.019
- (8) É.A. Souza Silva and J. Pawliszyn, *Anal. Chem.* **84**(16), 6933–6938 (2012). doi:10.1021/ac301305u
- (9) F.M. Musteata, M. Sandoval, J.C. Ruiz-Macedo, K. Harrison, D. McKenna, and W. Millington, *Anal. Chim. Acta* **933**, 124–133 (2016). doi:10.1016/j.aca.2016.05.053
- (10) F. M. Musteata, *TrAC Trends Anal. Chem.* **45**, 154–168 (2013).
- (11) N. Reyes-Garcés and E. Gionfriddo, *TrAC Trends Anal. Chem.* **113**, 172–181 (2019). doi:10.1016/j.trac.2019.01.009
- (12) B. Bojko, K. Gorynski, G.A. Gomez-Rios, J.M. Knaak, T. Machuca, V.N. Spetler, E. Cudjoe, M. Hsin, M. Cypel, M. Selzner, M. Liu, S. Keshavjee, and J. Pawliszyn, *Anal. Chim. Acta* **803**, 75–81 (2013). doi:10.1016/j.aca.2013.08.031
- (13) J.L. Harding and M.M. Reynolds, *Trends Biotechnol.* **32**(3), 140–146 (2014). doi:10.1016/j.tibtech.2013.12.004
- (14) J. L. Dalsin and P.B. Messersmith, *Mater. Today* **8**(9), 38–46 (2005). doi:10.1016/S1369-7021(05)71079-8
- (15) S. Lendor, S.A. Hassani, E. Boyaci, V. Singh, T. Womelsdorf, and J. Pawliszyn, *Anal. Chem.* **91**(7), 4896–4905 (2019). doi:10.1021/acs.analchem.9b00995
- (16) A. Napylov, N. Reyes-Garcés, G. Gomez-Rios, M. Olkowicz, S. Lendor, C. Monnin, B. Bojko, C. Hamani, J. Pawliszyn, and D. Vuckovic, *Angewandte Chemie* **59**(6), 2392–2398 (2020). doi:10.1002/anie.201909430
- (17) E. Cudjoe, B. Bojko, I. de Lannoy, V. Saldivia, and J. Pawliszyn, *Angewandte Chemie* **52**(46), 12124–12126 (2013). doi:10.1002/anie.201304538
- (18) B. Bojko, K. Gorynski, G.A. Gomez-Rios, J.M. Knaak, T. Machuca, E. Cudjoe, V.N. Spetler, M. Hsin, M. Cypel, M. Selzner, M. Liu, S. Keshavjee, and J. Pawliszyn, *Lab. Invest.* **94**, 586–594 (2014). doi:10.1038/labinvest.2014.44
- (19) N.T. Looby, M. Tascon, V.R. Acquaro, N. Reyes-Garcés, T. Vasiljevic, G.A. Gomez-Rios, M. Wasowicz, and J. Pawliszyn, *Analyst* **144**(12), 3721–3728 (2019). doi:10.1039/c9an00041k
- (20) E. Boyaci, B. Bojko, N. Reyes-Garcés, J.J. Poole, G.A. Gómez-Ríos, A. Teixeira, B. Nicol, and J. Pawliszyn, *Sci. Rep.* **8**(1), 1167 (2018). doi:10.1038/s41598-018-19313-1
- (21) N. Reyes-Garcés, M. N. Alam, and J. Pawliszyn, *Anal. Chim. Acta* **1001**, 40–50 (2018). doi:10.1016/j.aca.2017.11.014
- (22) N. Reyes-Garcés, M. Diwan, E. Boyaci, G.A. Gómez-Ríos, B. Bojko, J.N. Nobrega, F.R. Bambico, C. Hamani, and J. Pawliszyn, *Anal. Chem.* **91**(15), 9875–9884 (2019). doi:10.1021/acs.analchem.9b01540
- (23) J.J. Poole, J.J. Grandy, M. Yu, E. Boyaci, G.A. Gómez-Ríos, N. Reyes-Garcés, B. Bojko, H. Vander Heide, and J. Pawliszyn, *Anal. Chem.* **89**(15), 8021–8026 (2017). doi:10.1021/acs.analchem.7b01382
- (24) S. Lendor, S.A. Hassani, E. Boyaci, V. Singh, T. Womelsdorf, and J. Pawliszyn, *Anal. Chem.* **91**(7), 4896–4905 (2019). doi:10.1021/acs.analchem.9b00995
- (25) N. Reyes-Garcés, B. Bojko, D. Hein, and J. Pawliszyn, *Anal. Chem.* **87**(19), 9722–30 (2015). doi:10.1021/acs.analchem.5b01849
- (26) T. Vasiljevic, G.A. Gómez-Ríos, and J. Pawliszyn, *Anal. Chem.* **90**(1), 952–960 (2018). doi:10.1021/acs.analchem.7b04005
- (27) G.A. Gómez-Ríos and J. Pawliszyn, *Chem. Commun.* **50**(85), 12937–12940 (2014). doi:10.1039/C4CC05301J
- (28) G.A. Gómez-Ríos, E. Gionfriddo, J. Poole, and J. Pawliszyn, *Anal. Chem.* **89**(13), 7240–7248 (2017). doi:10.1021/acs.analchem.7b01553
- (29) G.A. Gómez-Ríos, T. Vasiljevic, E. Gionfriddo, M. Yu, and J. Pawliszyn, *Analyst* **142**(16), 2928–2935 (2017). doi:10.1039/c7an00718c
- (30) G.A. Gómez-Ríos, N. Reyes-Garcés, B. Bojko, and J. Pawliszyn, *Anal. Chem.* **88**(2), 1259–1265 (2016). doi:10.1021/acs.analchem.5b03668
- (31) A. Khaled, G.A. Gómez-Ríos, and J. Pawliszyn, *Anal. Chem.* **92**(8), 5937–5943 (2020). doi:10.1021/acs.analchem.0c00093
- (32) A. Kasperkiewicz, G.A. Gómez-Ríos, D. Hein, and J. Pawliszyn, *Anal. Chem.* **91**(20), 13039–13046 (2019). doi:10.1021/acs.analchem.9b03225
- (33) G.A. Gómez-Ríos, M. Tascon, N. Reyes-Garcés, E. Boyaci, J. Poole, and J. Pawliszyn, *Sci. Rep.* **7**(1) (2017). doi:10.1038/s41598-017-16494-z
- (34) M. Tascon, G.A. Gómez-Ríos, N. Reyes-Garcés, J. Poole, E. Boyaci, and J. Pawliszyn, *J. Pharm. Biomed. Anal.* **144**(10), 10.1016/j.jpba.2017.03.009 (2017). doi:10.1016/j.jpba.2017.03.009
- (35) G.A. Gómez-Ríos, M. Tascon, N. Reyes-Garcés, E. Boyaci, J.J. Poole, and J. Pawliszyn, *Anal. Chim. Acta* Accepted manuscript (2017).
- (36) S. Xiao, W. Cao, B. Wang, L. Xu, and B. Chen, *J. App. Polym. Sci.* **127**(4), 3198–3203 (2013). doi:10.1002/app.37733
- (37) E. Gionfriddo, D. Gruszecka, X. Li, and J. Pawliszyn, *Talanta* **211**(10), (2019), 120746 (2020). doi:10.1016/j.talanta.2020.120746
- (38) S. Risticicvic, E. A. Souza-silva, E. Gionfriddo, J.R. Deell, J. Cochran, W.S. Hopkins, and J. Pawliszyn, *Sci. Rep.* **10**(1), 1–11 (2020). doi:10.1038/s41598-020-63817-8
- (39) L. Zhang, E. Gionfriddo, V. Acquaro, and J. Pawliszyn, *Anal. Chim. Acta* **1031**, 83–97 (2018). doi:10.1016/j.aca.2018.05.066
- (40) S. De Grazia, E. Gionfriddo, and J. Pawliszyn, *Talanta* **167**, 754–760 (2017). doi:10.1016/j.talanta.2017.01.064
- (41) É.A. Souza-Silva, V. Lopez-Avila, and J. Pawliszyn, *J. Chromatogr. A* **1313**, 139–146 (2013). doi:10.1016/j.chroma.2013.07.071
- (42) V.F. Cardoso, D.M. Correia, C. Ribeiro, M.M. Fernandes, and S. Lanceros, *Polymers* **10**(2), 1–26 (2018). doi:10.3390/polym10020161
- (43) D. Lu and S. Weber, *J. Chromatogr. A* **1360**, 17–22 (2014). doi:10.1016/j.chroma.2014.07.060
- (44) E. Gionfriddo, E. Boyaci, and J. Pawliszyn, *Anal. Chem.* **89**(7) (2017). doi:10.1021/acs.analchem.6b04690
- (45) J. Pawliszyn, E. Gionfriddo, and E. Boyaci, Solid Phase Microextraction Coating. US Patent 10,545,077 B2 (2017).

Emanuela Gionfriddo is in the Department of Chemistry and Biochemistry at the School of Green Chemistry and Engineering at The University of Toledo, in Toledo, Ohio. Direct correspondence to: Emanuela.Gionfriddo@UToledo.edu

Boosting the Purification Process of Biopharmaceuticals by Means of Continuous Chromatography

Image credit: agsandrew/stock.adobe.com



Many biopharmaceuticals are currently purified by means of two or more successive single-column (batch) chromatographic steps. The first one is usually a *capture* step, which is used to remove non-product-related impurities, such as host-cell proteins and DNA. The second step is referred to as the *polishing* step, which removes product-related impurities, such as fragments and aggregates. However, single-column processes suffer some intrinsic limitations. Indeed, in the capture step, the trade-off between capacity utilization and productivity can be very relevant, while polishing processes are characterized by yield-purity trade-off. These limitations can be alleviated through continuous, or semi-continuous, countercurrent purification techniques. These processes display superior purification performance, allowing for the automated internal product recycling in the system composed of multiple identical columns, either interconnected or operated in parallel. In this paper, the advantages of capture simulated moving bed (captureSMB) for the capture step and multicolumn countercurrent solvent gradient purification (MCSGP) for polishing purposes will be illustrated.

Biopharmaceuticals have rapidly grown in popularity among the medical community in recent years, as a result of unprecedented advancements in biologics and human genetics. Due to their high affinity toward a specific molecule or receptor, biomolecule-based therapeutics have been proven to have very high efficacy even at low concentrations. Moreover, endogenous (or endogenous-like) biomolecules are better tolerated by human bodies than traditional therapeutics, preventing or diminishing the occurrence of side effects after their administration. For these reasons, biological drugs for the treatment of already existing and emerging diseases represent the basis for tomorrow's medicine.

The sudden outbreak of the COVID-19 pandemic disease caused by the new coronavirus 2019-nCoV (now officially designated as severe acute respiratory syndrome-related coronavirus, SARS-CoV-2), has led to an urgent demand for novel therapies for the treatment of clinically advanced conditions. Several options

can be taken into consideration for the treatment or prevention of COVID-19, mostly based on the use of biopharmaceuticals, including vaccines, monoclonal antibodies (mAbs), oligonucleotide-based therapies, peptides, interferon therapies and small-molecule drugs (1–4). Particularly relevant is the case of the mAb tocilizumab, under clinical evaluation for its ability to prevent the inflammatory process responsible for the worsening of pneumonia and pulmonary distress in patients affected by COVID-19 (4).

The industrial production of biopharmaceuticals has rapidly progressed in the last few years. However, the recent developments in cell culture and fermentation processes (such as for the production of mAbs) and solid-phase synthesis (for the production of peptides and oligonucleotides, for example) have not been matched by equivalent improvements in purification (downstream) processes, which often represent the bottleneck, in terms of both cost and time, in the entire production process (5).

Chiara De Luca, Simona Felletti, Giulio Lievore, Alessandro Buratti, Mattia Sponchioni, Alberto Cavazzini, Martina Catani, Marco Macis, Antonio Ricci, and Walter Cabri

Preparative liquid chromatography is the preferred method of choice to achieve the purified target at an acceptable degree of purity for therapeutics (6,7). Most of the modern downstream processes need at least two single-column purifications. The first one is usually called *capture* step, which serves to remove all non-product-related impurities, such as host-cell proteins and DNA. Successive *polishing* steps are then used to obtain the target at the desired degree of purity, by removing all product-related impurities. These are species, produced during the synthesis, with very similar chemical characteristics to the target compound (such as, truncated or deamidated species and aggregates, for example). The removal of these impurities via chromatography is very challenging, because their chromatographic behavior is often similar to that of the target. This situation very often leads to overlapping regions in the chromatogram where target and impurities are coeluted. The collection of these regions improves the yield of the separation at the expense of the overall purity. On the other hand, the discharge of these regions saves the overall purity at expenses of the process yield. These considerations are at the basis of the well-known purity-yield trade-off, affecting the performance of elution chromatography.

Among the strategies that can enhance the downstream process, multicolumn countercurrent continuous, or semi-continuous, chromatographic techniques seem to be particularly suitable. One of the greatest advantages of continuous techniques is that the purification process can be completely automated, with no human intervention, with a considerable saving of time. These approaches involve the use of two (or more) “identical” columns of the same dimensions and stationary phase, connected through a series of valves. This system allows not only the internal product recycling of the overlapping regions for enhanced product-impurity separation, but also to simulate the apparent opposite movement of the stationary phase with respect to the mobile one, from where the term *countercurrent* is derived to refer to these techniques.

The countercurrent separation of two compounds can be explained through the simple graphic represented in Figure 1. Let us imagine that a slower turtle and a faster

rabbit are moving in the direction of the blue arrow (right). Suddenly, they fall onto a conveyor belt moving in the opposite direction (left). Depending on the relative velocities of the turtle and the rabbit (compared to that of conveyor belt that can be properly varied), the slow turtle will be transported to the left of the conveyor belt, while the fast rabbit will continue its run to the right. At the end, the two animals will be separated at the opposite sides of the conveyor belt. In this representation, the turtle is the strongly adsorbed compound (slower velocity into the column), while the rabbit is the weakly adsorbed one (moving faster). The blue arrow represents the direction of the mobile phase. Finally, the conveyor belt represents the countercurrent movement of the stationary phase.

The first countercurrent multicolumns setup was simulated moving bed (SMB) applied for the first time more than 60 years ago for the separation of binary mixtures (8–11). Since then, the SMB concept has been modified and improved, particularly in the direction of reducing the number of columns connected together. This paper focuses, in particular, on two of the most recent improved versions of the traditional SMB concept, captureSMB and multicolumn countercurrent solvent gradient purification (MCSGP). Their advantages over traditional single-column techniques for the purification of therapeutic biomolecules are illustrated.

CaptureSMB

The capture step usually deals with very large volumes of feed coming from the upstream process containing a large number of non-product-related impurities. An affinity resin is used to selectively capture the target molecule. All the other impurities will not bind to the stationary phase, and, therefore, they can be easily removed.

Let us consider a typical case where capture processes are employed—the purification of mAbs with Protein A stationary phase (12). In batch chromatography, the feed is injected into the column by adjusting the loading on the base of the dynamic binding capacity (DBC) value, which can be experimentally evaluated by a breakthrough curve (see Figure 2). A 1% DBC (the capacity at 1% of the breakthrough curve) is taken as reference limit to indicate the saturation of all available affinity

sites on the stationary phase. By loading the column beyond this limit, there would be a loss of the target, which would not bind to the stationary phase. Therefore, in batch processes, the column is usually loaded up to 80–90% of 1% DBC, with a 10–20% margin in order to avoid any target-compound loss. After the loading, the target is eluted from the column and the resin is washed and regenerated.

Even if very high yield and purity can be obtained by means of batch purifications, there is an intrinsic trade-off between capacity utilization and productivity. Capacity utilization (*CU*) is defined as the ratio between the loading (*L*) and the maximum saturation capacity of the stationary phase (Q_{sat}), which also corresponds to the static binding capacity (SBC):

$$CU\% = \frac{L}{Q_{sat}} \times 100 \quad [1]$$

Productivity (for an *n*-column process) is defined as:

$$Prod\% = \frac{m_{target\ recovered}}{t_{run} \times n \times V_{col}} \times 100 \quad [2]$$

where $m_{target\ recovered}$ is the mass of the target collected at the end of the run, t_{run} is the duration of a run and V_{col} is the geometrical volume of the column. For a batch process, $n = 1$. Productivity is expressed in g/L/h.

To explain the trade-off of batch capture processes, it must be considered that capacity utilization can be increased by changing the DBC value. Indeed, higher DBC values can be obtained by steepening the breakthrough curve. This can be achieved by decreasing the loading flow velocity. However, lowering the loading flow velocity negatively impacts productivity, which will be unavoidably decreased (besides, buffer consumption increases).

This trade-off can be alleviated by employing multicolumn countercurrent processes (7). One of the most modern approaches for the capture step in semi-continuous mode is captureSMB. In its simplest version, two identical columns (packed with Protein A resin in the case of mAb purification) are connected through a series of valves. It is a quite complex process that can be

Table I: Equation for capacity utilization calculation in batch and captureSMB processes. Capital letters refers to areas shown in Fig. 2.

CU% batch	CU% captureSMB
$\frac{A}{A+B+D} \times 100$	$\frac{A+B}{A+B+D} \times 100$

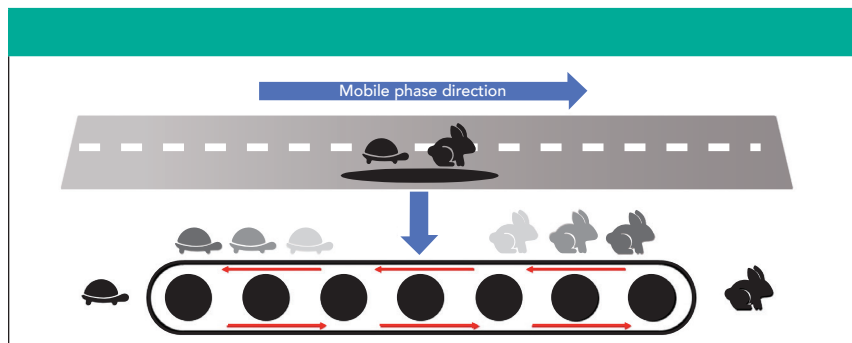


Figure 1: Schematic representation of the countercurrent mechanism; see text for details. Shadowed images of the turtle and the rabbit serve to simulate their movements. Modified with permission from reference (7).

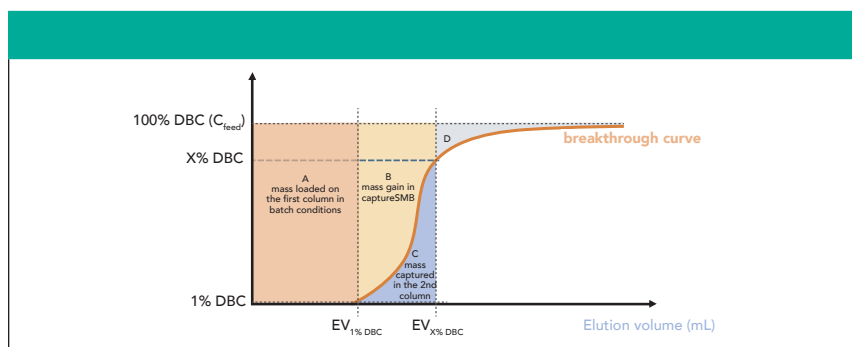


Figure 2: Schematic representation of a breakthrough curve. Area A represents the mass that can be loaded in the first column in batch conditions to reach 1% DBC. In twin-column captureSMB, the mass loaded on the first column is given by $A + B$ while mass C is captured on the second column. The maximum saturation capacity of the stationary phase is given by the sum of masses $A + B + D$. $EV_{1\% \text{ DBC}}$ and $EV_{X\% \text{ DBC}}$ are the elution volumes at 1% and X% DBC, respectively.

briefly summarized in the steps represented in Figure 3. Interested readers are referred to references (13–15) for a comprehensive description.

As it can be seen from Figure 3, there are moments when columns are sequentially loaded and washed (so-called interconnected steps), and others where columns are not connected to each other (batch steps). During batch steps, one column is washed, eluted, and regenerated, while loading is continued on the other. A full cycle is completed when the two columns turn back in their initial position. What is worth mentioning is that captureSMB makes it possible to drastically increase capacity utilization. A schematic representation is given in Figure 2, where a

hypothetical breakthrough curve is represented. In batch chromatography, only the mass represented by area A is loaded on the column. This corresponds to the mass that can be loaded before 1% DBC.

In twin-column captureSMB, the loading can be increased. Therefore, the first column is loaded up to a X% DBC (usually 70% DBC), containing the mass corresponding to $A + B$ in Figure 2, while mass in area C (breaking through from the first column) will be captured in the second column. The total $A + B + D$ area corresponds to the maximum saturation capacity, Q_{sat} . Thus, according to this scheme, capacity utilization for the two processes can be expressed, as reported in Table I.

As an example, captureSMB showed an increase of +26% in productivity and +11% in capacity utilization at a linear velocity of 150 cm/h for the purification of an IgG1 antibody on Amsphere JWT-203 protein A resin (16). The outcome was even better at 600 cm/h, with increases of +35% and +41% for productivity and capacity utilization, respectively. These results indicate a further advantage of captureSMB over batch processes, that is the possibility of operating at higher linear velocities since loadings are performed at much higher values than 1% DBC.

Another example is reported in (17), where mAb fragments have been purified in captureSMB by using a Capto L resin. Here, results showed a clear advantage of captureSMB over the correspondent batch process by achieving a +60% increase in loading, a +93% higher productivity, and a -54% in buffer consumption.

Multicolumn Countercurrent Solvent Gradient Purification (MCSGP)

Differently from the capture step, polishing is needed to remove all product-related impurities, including, but not limited to, isoforms, truncates, aggregates, and deamidates. These impurities are usually produced during the synthesis, and they usually have very similar chromatographic characteristics to those of the target. The presence of product-related impurities can generate several peak overlapping regions in the chromatogram, where slightly weaker, W, and slightly stronger, S, adsorbing impurities are co-eluted with the front and the rear part of the peak of the target product, P (see Figure 4). In these cases, batch purifications are most likely governed by a yield-purity trade-off. This means that, in order to obtain a pool with acceptable purity for pharmaceutical standards, the collection window need to be narrowed at the cost of yield (and vice versa). To avoid wasting considerable amounts of target product, the overlapping regions (where the target component is still present but with an excessive amount of impurities) are manually recycled and reprocessed. This is a very labor-intensive activity that tremendously impacts on the productivity of the process.

The yield-purity trade-off can be alleviated by employing multicolumn coun-

tercurrent techniques. Among these, the multicolumn countercurrent solvent gradient purification (MCSGP) is a semi-continuous process suitable for the challenging purification of complex mixtures, that also permits the use gradient elution (18–21). This is particularly interesting for the separation of large biomolecules, whose retention is strongly affected by the organic modifier concentration (20,22–24). In Figure 3, the principles of MCSGP, in the case of a ternary separations, are schematically depicted. As in captureSMB, also in MCSGP two (or more) identical columns are used.

Differently from captureSMB, where recycling occurs during loading, in MCSGP instead recycling takes place during elution (see Figure 5). Indeed, the feed is loaded on the first column, the overlapping regions (W/P and P/S) are recycled on the second column while the purest fraction of product (P) is collected from the first one. Then the second column is fed with fresh feed, in order to keep the loading constant, and the elution starts now from the second column to the first one. One cycle ends when the two columns turn back in their initial position. The process runs in a cyclic way, and a steady state is reached where purity and recovery do not change cycle after cycle. This mechanism partially overcomes the yield-purity trade-off usually faced in batch separations. Indeed, the recycling of overlapping regions can increase the yield of the collected product while maintaining purity that is at least equivalent to that of a batch process (product purity strictly depends on the pooling criteria). The interested reader can find a detailed description of the process in references (12,25,26–28).

MCSGP has been successfully applied to the purification of many classes of biomolecules. Different chromatographic media can be used in MCSGP, ranging from reversed-phase columns for the purification of peptides (25) to ion-exchange for the purification of oligonucleotides (29) or mAb charge variants (21,30).

It is worth mentioning that even a small increase in yield can be very advantageous when dealing with very expensive biopharmaceuticals. For example, references (21,30) report the purification of charged variants of mAbs with MCSGP on an ion-exchange column. An increase in yield

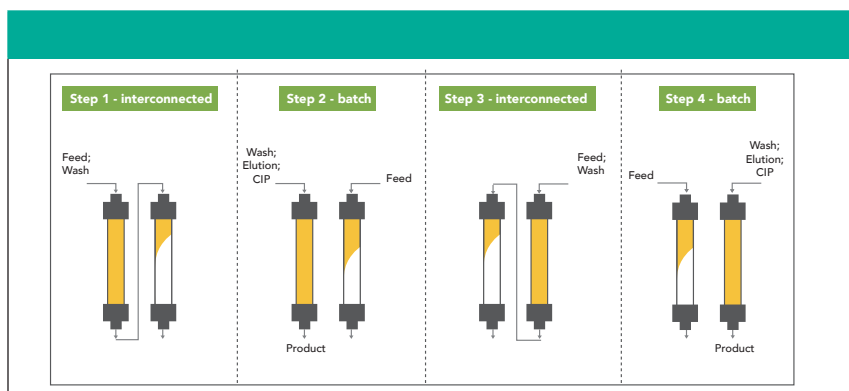


Figure 3: Schematic representation of twin-column captureSMB process. CIP stands for cleaning-in-place.

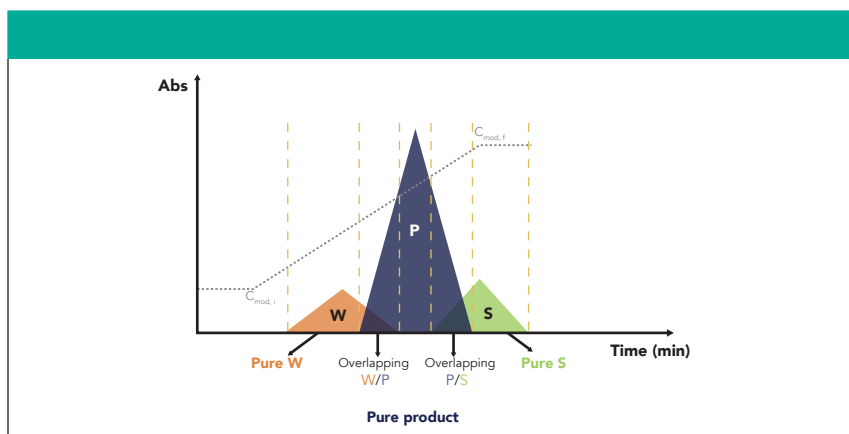


Figure 4: Schematic illustration of a ternary separation where the chromatographic peak of the target product (P) partially overlaps with those of two product related impurities. Here W refers to weakly adsorbing impurities and S to strongly adsorbed ones. Dotted grey line represents a hypothetical gradient of the modifier from an initial concentration $C_{mod, i}$ to a final concentration $C_{mod, f}$.

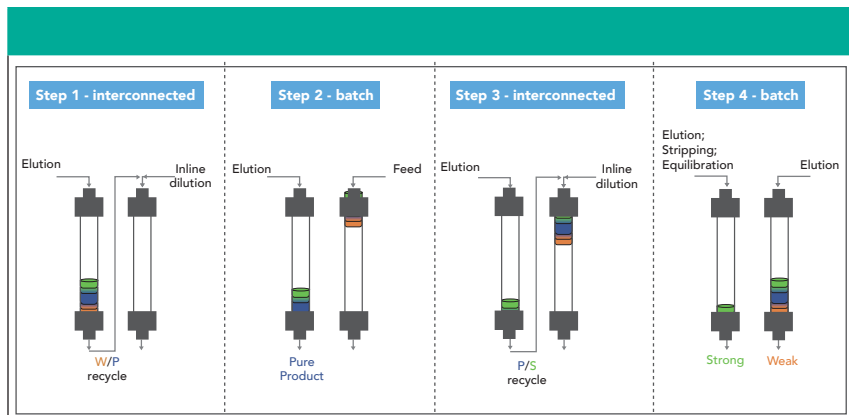


Figure 5: Schematic illustration of a twin-column MCSGP process.

of +56% and +74% was observed for the purification of bevacizumab (used for the treatment of many cancer diseases) and trastuzumab (used for the treatment of breast cancer), respectively, by maintaining purity constant with respect to batch purifications (30). Also, the purification process of oligonucleotides can be boosted

through MCSGP. Indeed, the yield in the purification of a mixture of oligonucleotides on HiScreen Q Sepharose FF columns was increased from 60% to 91% by moving from batch to MCSGP, maintaining the purity at 92% (29). Recently, some of the authors of this paper have applied the MCSGP process to the purification of

a therapeutic peptide from solid-phase synthesis on a C8 stationary phase (25), allowing for a +23% yield compared to the batch process, with an unchanged purity of 89%.

Conclusions and Future Perspectives

Continuous, or semi-continuous, countercurrent techniques make it possible to partially overcome common limitations of current single-column purification strategies that often represent a bottleneck of the whole production process. CaptureSMB makes it possible to increase both capacity utilization of the resin and productivity for the capture process, making it possible to operate also at faster linear velocities than correspondent batch processes. This technique is particularly suitable for the purification of mAbs on Protein A stationary phases, but it can be used with any other affinity system (for example, protein-ligand). On the other hand, MCSGP permits to alleviate the yield-purity trade-off typical of polishing batch processes by allowing for the internal recycling of overlapping regions of the chromatogram where the target is still present in a considerable amount but polluted with impurities. This technique has been successfully applied for the purification of peptides, oligonucleotides, and charge variants of mAbs, but it can be used for any other class of biomolecules.

The greatest advantage of these techniques is that, once the experimental conditions have been optimized, the purification process can be completely automated. Therefore, no human intervention is required to process large quantities of material.

Thanks to these advantages, multicolumn countercurrent techniques represent a convenient alternative over traditional batch purification processes for the ongoing development of novel therapeutics, vaccines, and monoclonal antibody therapies for the treatment of many diseases, including pandemic COVID-19.

Acknowledgments

The authors thank the Italian University and Scientific Research Ministry (grant PRIN2017Y2PAB8003, "Cutting edge analytical chemistry methodologies and

bio-tools to boost precision medicine in hormone-related diseases").

References

- (1) G. Li and E. De Clercq, *Nat. Rev.* **19**, 149–150 (2020).
- (2) J.S. Morse, T. Lalonde, S. Xu, and W.R. Liu, *ChemBioChem* **21**, 730–738 (2020).
- (3) C. Liu, Q. Zhou, Y. Li, L.V. Garner, S.P. Watkins, L.J. Carter, J. Smoot, A.C. Gregg, A.D. Daniels, S. Jervey, and D. Alibai, *ACS Cent. Sci.* **6**, 315–331 (2020).
- (4) E. Nicastrì, N. Petrosillo, T. Ascoli Bartoli, L. Lepore, A. Mondì, F. Palmieri, G. D'Offizi, L. Marchioni, S. Muratelli, G. Ippolito, and A. Antinori, *Infect. Dis. Rep.* **12**:8543, 3–9 (2020).
- (5) A.A. Shukla and J. Thömmes, *Trends Biotechnol.* **28**, 253–261 (2010).
- (6) G. Guiochon, A. Felinger, A. Katti, and D. Shirazi, *Fundamentals of Preparative and Non-linear Chromatography* (Academic Press, Boston, Massachusetts, 2nd Ed., 2006).
- (7) G. Subramaniam, *Continuous Processing in Pharmaceutical Manufacturing* (Wiley-VCH Verlag GmbH & Co. KGaA, Weinheim, Germany, 1st Ed., 2015).
- (8) M. Mazzotti, G. Storti, and M. Morbidelli, *J. Chromatogr. A* **769**, 3–24 (1997).
- (9) E. R. Francotte and P. Richert, *J. Chromatogr. A* **1997**, 101–107 (1997).
- (10) H. Schramm, M. Kasperit, A. Kienle, and A. Seidel-Morgenstern, *J. Chromatogr. A* **1006**, 77–86 (2003).
- (11) [T. Kröber, M. W. Wolff, B. Hundt, A. Seidel-Morgenstern, and U. Reichl, *J. Chromatogr. A* **1307**, 99–110 (2013)
- (12) B. Kelley, *Biotechnol. Progr.* **23**, 995–1008 (2007).
- (13) F. Steinebach, T. Müller-Späh, and M. Morbidelli, *Biotechnol. J.* **11**, 1126–1141 (2016).
- (14) J. Angelo, J. Pagano, T. Müller-Späh, K. Mithlbachler, S. Chollangi, X. Xu, S. Ghose, and Z. J. Li, *BioProcess Intl.* **16**(4), 1–6 (2015).
- (15) M. Angarita, T. Müller-Späh, D. Baur, R. Lievrouw, G. Lissens, and M. Morbidelli, *J. Chromatogr. A* **1389**, 85–95 (2015).
- (16) T. Müller-Späh, M. Angarita, D. Baur, M. Morbidelli, R. Lievrouw, M. Bavand, G. Lissens, and G. Strohlein, *Biopharm Intl.* **26** (2013).
- (17) C. Grossman, G. Ströhlein, M. Morari, and M. Morbidelli, *J. Proc. Control* **20**, 618–443 (2010).
- (18) W. Jin and P. C. Wankat, *Ind. Eng. Chem. Res.* **44**, 1565–1575 (2005).
- (19) A. L. Zydney, *Biotech. Bioeng.* **113**, 465–475 (2016).
- (20) G. Ströhlein, L. Aumann, M. Mazzotti, and M. Morbidelli, *J. Chromatogr. A* **1126**, 338–346 (2006).
- (21) T. Müller-Späh, L. Aumann, L. Melter, G. Ströhlein, and M. Morbidelli, *Biotech. Bioeng.* **100**, 1166–1177 (2008).
- (22) N. Marchetti, F. Dondi, A. Felinger, R. Guerini, S. Salvadori, and A. Cavazzini, *J. Chromatogr. A* **1079**, 162–172 (2005).
- (23) D. Åsberg, M. Léso, T. Leek, J. Samuelsson, K. Kaczmarek, and T. Fornstedt, *Chromatographia* **80**, 961–966 (2017).
- (24) C. De Luca, S. Felletti, M. Macis, W. Cabri, G. Lievore, T. Chenet, L. Pasti, M. Morbidelli, A. Cavazzini, M. Catani, and A. Ricci, *J. Chromatogr. A* <https://doi.org/10.1016/j.chroma.2019.460789> (2020).
- (25) C. De Luca, S. Felletti, G. Lievore, A. Buratti, S. Vogt, M. Morbidelli, A. Cavazzini, M. Catani, M. Macis, A. Ricci, and W. Cabri, submitted to *J. Chromatogr. A* (2020).
- (26) D. Pfister, L. Nicoud, and M. Morbidelli, *Continuous Biopharmaceutical Processes-Chromatography: Bioconjugation and Protein Stability* (Cambridge Series in Chemical Engineering, Cambridge University Press, Cambridge, UK, 2018).
- (27) L. Aumann and M. Morbidelli, *Biotech. Bioeng.* **98**, 1043–1055 (2007).
- (28) [28] F. Steinebach, N. Ulmer, L. Decker, L. Aumann, and M. Morbidelli, *J. Chromatogr. A* **1492**, 19–26 (2017).
- (29) Application Note. P2.V1, https://www.chromacon.com/resources/public/lava3/media/kcfinder/files/Oligonucleotide_MCSGP_application_note.pdf (2019).
- (30) T. Müller-Späh, M. Krätli, L. Aumann, G. Ströhlein, and M. Morbidelli, *Biotech. Bioeng.* **107**, 652–662 (2010).

Chiara De Luca, Simona Felletti, Giulio Lievore, Alessandro Buratti, Alberto Cavazzini and Martina Catani are with the Dept. of Chemistry and Pharmaceutical Sciences, at the University of Ferrara, in Ferrara, Italy. **Mattia Sponchioni** is with the Dept. of Chemistry, Materials and Chemical Engineering at the Politecnico di Milano, in Milan, Italy. **Marco Macis, Antonio Ricci and Walter Cabri** are with the Fresenius Kabi iPSUM, in Rovigo, Italy. **Walter Cabri** is also with the Department of Chemistry at the University of Bologna, in Bologna, Italy. Direct correspondence to: martina.catani@unife.it



SELECTRA® U/HPLC Columns

Reproducible, Robust & Selective

Bringing Our Superior
Phases to you
in U/HPLC Format



DA – Unique Polyaromatic Phase

C18 – Traditional Reverse Phase

Aqueous C18 – Traditional Reverse Phase with Enhanced Selectivity

C8 – Less Retentive than Standard C18 Column

PFPP – Operates in Reverse Phase, Normal Phase, or HILIC Mode

EtG – Maximum retention for polar EtG/EtS alcohol metabolites

Available in 1.8, 3, and 5µm particle sizes

800.385.3153 www.unitedchem.com

Antibody Analysis with (U)HPLC

